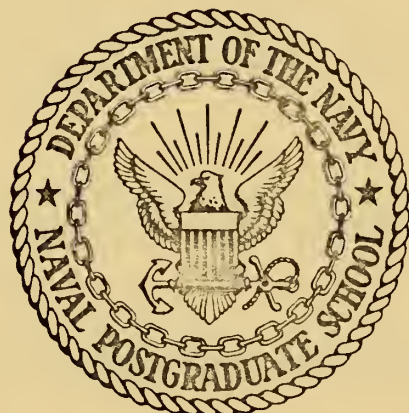


THE DEVELOPMENT AND STUDY OF A
MATHEMATICAL MODEL FOR NON-CATALYTIC
REACTIONS IN A FLUIDIZED BED REACTOR

Charles Joseph Dale

NAVAL POSTGRADUATE SCHOOL

Monterey, California



THESIS

THE DEVELOPMENT AND STUDY OF A
MATHEMATICAL MODEL FOR NON-CATALYTIC
REACTIONS IN A FLUIDIZED BED REACTOR

by

Charles Joseph Dale

Thesis Advisor:

J. H. Duffin

June 1972

Approved for public release; distribution unlimited.

The Development and Study of a Mathematical Model
for
Non-catalytic Reactions in a Fluidized Bed Reactor

by

Charles Joseph Dale
Ensign, United States Navy
B.E., Villanova University, 1971

Submitted in partial fulfillment of the
requirements for the degree of

MASTER OF SCIENCE IN CHEMISTRY

from the
NAVAL POSTGRADUATE SCHOOL
June 1972



ABSTRACT

A mathematical model for the simulation of non-catalytic solid-gas reactions in a fluidized bed reactor is proposed. The performance of the model in predicting solid reactant conversions for an ore roasting process is investigated using available literature data. Model development required simplifying assumptions. The sensitivity of the model to certain of these assumptions is investigated.

Comments on the adaptability of the model for use in the design and study of a fluidized bed shipboard waste disposal system are made.

TABLE OF CONTENTS

I.	INTRODUCTION -----	12
II.	LITERATURE SEARCH -----	13
III.	MODEL DEVELOPMENT -----	19
	A. OVERALL BED MODEL -----	21
	1. Bubble Size and Section Height Calculation -----	21
	2. Bed Voidage and Height Calculation -----	25
	B. SECTION MODEL -----	26
	1. Bubble Phase Description -----	26
	2. Cloud and Wake Description -----	28
	3. Emulsion Description -----	29
	4. Solid Movement and Gas Exchange -----	29
	C. KINETICS -----	31
	D. MATERIAL BALANCES -----	33
	1. Preliminary Assumptions -----	33
	2. Section Material Balances -----	35
	3. Solution of the Material Balance Equations -----	40
	a. Calculation for the Top Section -----	40
	b. Calculation for the (N-1) th Section -----	44
	c. Calculation for the Feed Section -----	45
	E. THE COMPUTER MODEL -----	47
IV.	PRESENTATION AND DISCUSSION OF RESULTS -----	50
	A. OVERALL RESULTS: GENERAL MODEL PERFORMANCE -----	50

B. EFFECTS OF THE MAJOR ASSUMPTIONS -----	52
1. Modified Section Height Calculation -----	52
2. Backmixing Considerations -----	57
3. Analysis of the Initial Reactor Section -----	61
V. CONCLUSIONS AND RECOMMENDATIONS -----	72
APPENDIX A: TERMINAL VELOCITY CALCULATION -----	74
APPENDIX B: CHARACTERISTICS AT MINIMUM FLUIDIZATION -----	75
APPENDIX C: DATA FOR THE CALCULATION OF THE WAKE VOLUME -----	78
APPENDIX D: COMPUTER INPUT DATA -----	79
APPENDIX E: MODIFIED SECTION HEIGHT CALCULATION -----	80
COMPUTER PROGRAM -----	81
BIBLIOGRAPHY -----	96
INITIAL DISTRIBUTION LIST -----	100
FORM DD 1473 -----	101

LIST OF TABLES

I.	Second Generation Fluidized Bed Models -----	17
II.	Computer Input Variables -----	48
III.	Major Computer Program Sections -----	49
IV.	Comparison of Overall Results with Literature Data -----	51
V.	Predicted Conversions for Model with Section Height Based on the Cloud Diameter -----	56
VI.	Results of Conversion Calculations from Backmixed Equations -----	60
VII.	Solid Concentration Data for the Initial Section -----	63
VIII.	Input Data -----	79

LIST OF FIGURES

1.	Six Parameter Two Phase Model -----	14
2.	States of the Gas-solid System -----	20
3.	Sectionalized Model of the Fluid Bed Reactor -----	22
4.	Averaging Procedure Used to Determine Sections Heights -----	24
5.	Bubble Representation -----	27
6.	Shrinking Core Reaction Model -----	32
7.	Core Size Distribution -----	34
8.	Radial Solid Concentration Profile -----	36
9.	Section Gas Flow Representation -----	37
10.	Top Section Modification -----	39
11.	Flow Streams for Overall Material Balances -----	41
12.	Top Section Material Balances -----	43
13.	Flow Chart for the Solution of the Material Balances -----	46
14.	Section Height Based on Bubble Size -----	53
15.	Gas Concentration Profiles for Run 12; ΔH_1 Based on Bubble Size -----	55
16.	Exit Age Distribution -----	59
17.	Gas Concentration Profiles for Run 1; ΔH_1 Based on Cloud Size -----	64
18.	Gas Concentration Profiles for Run 12; ΔH_1 Based on Cloud Size -----	65
19.	Conversion Versus ΔH_1 Runs 1, 12 -----	67
20.	Normalized Gas Concentration Profiles Runs 10, 11, 12 -----	68

21.	Conversion Versus ΔH_1 Runs 10, 11, 12 -----	70
22.	EMF Data -----	76
23.	Plot of Data for Determination of the Wake Volume -----	78

TABLE OF SYMBOLS

A_{rx}	reaction area per particle, ft. ²
b	stoichiometric coefficient
\bar{C}_g	average gas concentration, moles/ft. ³
C_{GB}	bubble phase gas concentration, moles/ft. ³
C_{GE}	emulsion phase gas concentration, moles/ft. ³
C_{G_0}	initial gas concentration, moles/ft. ³
C_{S}	reactant concentration in the solid, moles/ft. ³
C_{S_0}	initial reactant concentration in the solid, moles/ft. ³
D_b	axial dispersion coefficient for the reactant in the bubble phase, ft. ² /sec
D_B	bubble diameter, in.
D_B_{avg}	average bubble diameter, in.
D_B_{max}	maximum bubble diameter, ft.
D_C	cloud diameter, in.
D_e	axial dispersion coefficient for the reactant in the emulsion, ft. ² /sec
DIFH	residual height in the top section, in.
D_o	initial bubble size, in.
D_p	diameter of the bed particles, ft.
$E(t)$	exit age distribution function
f	volumetric fraction of gas flow in the emulsion phase, l/sec
F	volumetric fraction of gas flow in the bubble phase, l/sec
g	acceleration of gravity, ft./sec ²
H	total bed height, in.

HMF	height of bed at minimum fluidization, in.
H_o	minimum height of bed ($\varepsilon=0$), ft.
K_{be}	gas exchange coefficient based on bubble volume, 1/sec
k_c	kinetic rate constant, ft./sec
K_r	kinetic rate constant based on a unit volume of solids, 1/sec.
M	molecular weight of the gas, lbs./mole
N	number of bubbles
N_a	moles of component A, moles
N_o	number of holes per square ft. in the distributor plate, ft. ⁻²
P	pressure, lbs./ft. ²
R	gas law constant
R_B	bubble radius, in.
R_c	core radius (Rcore), ft.
R_{cl}	cloud radius, in.
Re	Reynold's Number
S_B	area of the bubble phase, in. ²
S_T	cross sectional area of the reactor, in. ²
t	time, sec
\bar{t}	average particle residence time, sec
T	reactor temperature, °F
T'	reactor temperature, °K
T_B	normal boiling point, °K
U	superficial gas velocity at the bed temperature, ft./sec
U_{BR}	absolute bubble rise velocity, ft./sec
U_{BREL}	relative bubble rise velocity, ft./sec

U_e	superficial gas velocity in the emulsion, ft./sec
UMF	minimum fluidization velocity at the bed temperature, ft./sec
UMF_0	minimum fluidization velocity at room temperature (20°C), ft./sec
U_o	superficial gas velocity at room temperature (20°C), ft./sec
U_T	particle terminal velocity, ft./sec
U_{vol}	gas volumetric flow rate, ft^3/sec
VB	bubble phase volume, in^3
VB_{FR}	fractional bubble phase volume in the top section, in^3
VB_T	total bubble volume in the bed, in^3
VB_1	volume of one bubble in the top section, in^3
VC	cloud phase volume, in^3
V_{core}	volume of the unreacted core, ft^3
VE	emulsion phase volume, in^3
V_{FR}	fractional cloud-bubble volume in the top section, in^3
Vo	initial volume of a single particle, ft^3
VT_1	volume of one bubble and cloud in the top section, in^3
VW	volume of the wake, in^3
WB	bubble phase solid flow, ft^3/sec
WE	emulsion phase solid flow, ft^3/sec
w_f	volumetric feed rate of solids, ft^3/sec
w_t	weight of solids in the bed, lbs.
XB	solid reactant conversion
X_m	constant - $0.684 \rho p D_p$, in.
y_i	mole fraction of gas i
α	ratio of wake to bubble volume

ϵ	bed voidage
ϵ_{MF}	bed voidage at minimum fluidization
γ_c	solid distribution coefficient in the cloud and wake, ft^3
γ_e	solid distribution coefficient in the emulsion phase, ft^3
μ_i	viscosity of gas i, centipoise
μ'	viscosity of gas, lbs./ft.sec
μ_{mix}	viscosity of the gas mixture, centipoise
ρ_g	gas density, lbs./ft.^3
ρ_p	particle density, lbs./ft.^3
ρ_p'	molar particle density, moles/ ft.^3
τ	time for complete reaction, sec

I. INTRODUCTION

In the late sixties, the Navy began a study of shipboard waste disposal systems which could be used to combat a growing pollution problem. One proposal considered a process for the combustion of solid waste material in a fluidized bed reactor. This proposal was opposed by some naval designers on the grounds that sufficient knowledge of the operational characteristics of fluid bed reactors was not available, thus prohibiting accurate design and control of such a system.

This lack of fundamental design knowledge is a problem which has plagued fluid bed technologists for some time. Although the fluid bed reactor finds broad usage in the chemical industry today, its complex nature makes accurate mathematical modeling difficult. Design and control of fluid bed systems in the past has, therefore, been based on the application of operational engineering experience.

This work was undertaken with the goal of studying and developing a mathematical model of a fluidized bed reactor. The Bubble Assemblage Model proposed by Wen and Yoshida [1] provided the starting point for this investigation.

If a reasonable model could be developed, it could be used as a design tool and in studies of the operational characteristics of the reactor system.

II. LITERATURE SEARCH

Early tracer studies [2] on large scale fluid bed reactors revealed that tracer concentrations in the exit gas stream exceeded concentrations in samples taken directly from the bed. This observation led to the development of the two phase model of fluidization which predicts that the major portion of the gas passes through the bed in the form of bubbles. The primary developers of this theory include Toomey and Johnstone [3], Shen and Johnstone [4], Pansing [5], and Lewis et al [6].

The two phase model pictures the bed as consisting of two single phase reactors in parallel as shown in Figure 1. Phase 1, the lean or bubble phase, represents the primary means of gas throughput. It is generally treated as being in plug flow and containing no solids. Phase 2, the dense or emulsion phase, contains the solids surrounded by interstitial gas. Assumptions on the mixing patterns in the emulsion phase range depending on the investigator. Mathias and Watson [7], Massimillia and Johnstone [8], and Gomez-plata and Shuster [9] assumed plug flow behavior while Shen and Johnstone [4] and Lewis et al [6] have studied conditions of plug flow and complete mixing. The model is also characterized by a gas exchange coefficient which accounts for gas flow between the phases.

May [10] extensively studied the classic two phase model and was the first to introduce diffusion type coefficients

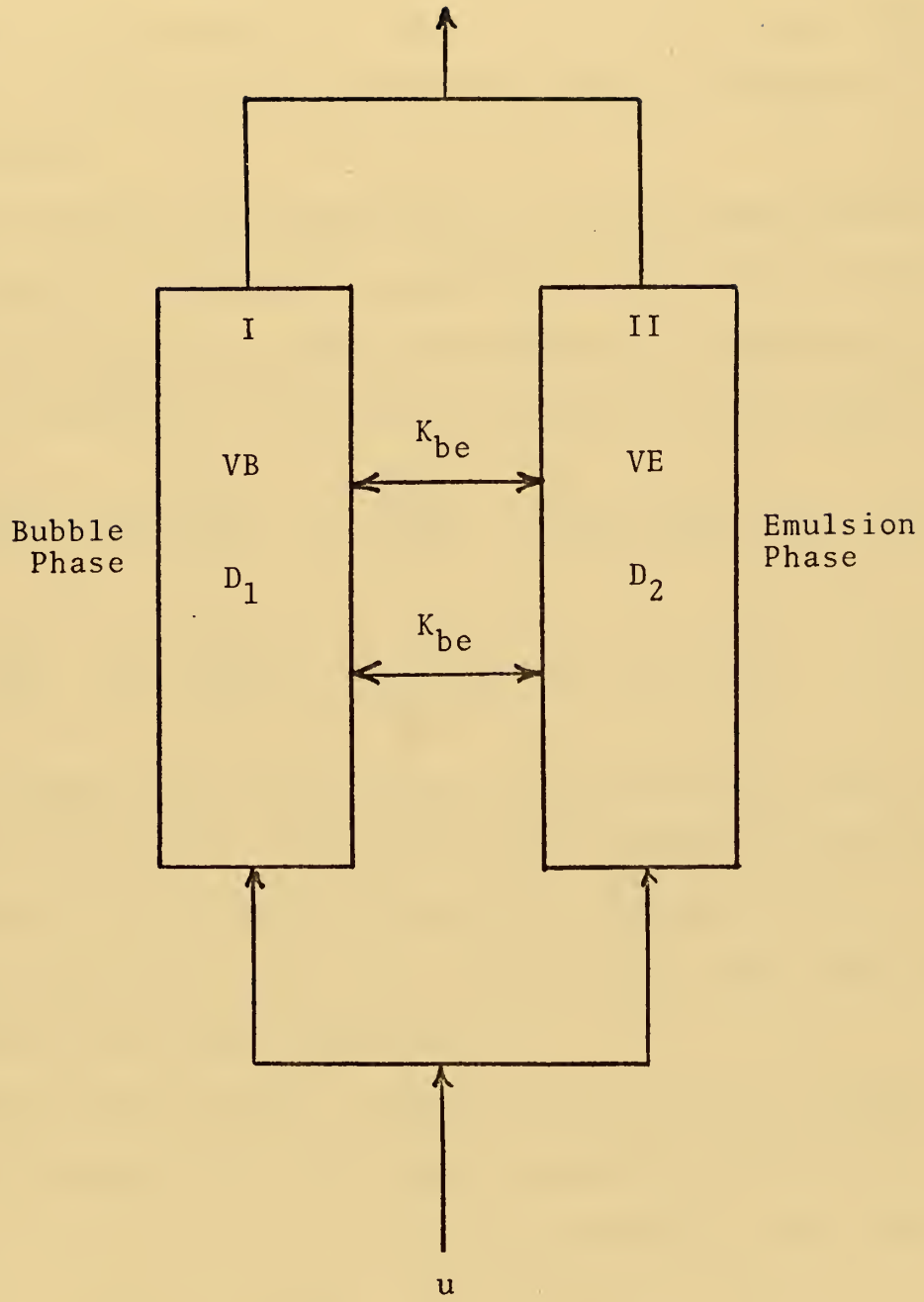


Figure 1. Six Parameter Two Phase Model.

to characterize the vigorous mixing in the emulsion phase. This approach was investigated further by van Deemter [11] who applied the model in a study of gas mixing experiments in order to determine the diffusion and gas exchange coefficients.

The mathematical formulation of the two phase model leads to two partial differential equations containing six parameters and representing the system material balances. A general expression of the model equations can be given as

$$F \frac{\partial C_{GB}}{\partial t} - F D_b \frac{\partial^2 C_{GB}}{\partial t^2} + F U \frac{\partial C_{GB}}{\partial H} + F_o (C_{GB} - C_{GE}) = 0 \quad (1)$$

$$f \frac{\partial C_{GE}}{\partial t} - f D_e \frac{\partial^2 C_{GE}}{\partial t^2} + f U_e \frac{\partial C_{GE}}{\partial H} + F_o (C_{GE} - C_{GB}) = 0 \quad (2)$$

Their solution has been a center of controversy because of different approaches to the choice of boundary conditions. McCracken [12] obtained solutions for various mixing patterns and in a second work [13] reviews other numerical solutions of the model equations.

The two phase model, although representing a useful engineering approach to the understanding of fluid bed reactors, suffers from serious disadvantages. The model parameters are, in a sense, adjustable and, therefore, while fitting experimental data well for particular cases, their generality for use in scale up and design are questionable. Furthermore, the description of a uniform bubble phase and constant gas exchange coefficient ignores effects of changing bubble size on bed operation.

Pioneering work in development of a more general model was completed by Davidson and Harrison [14] in 1962. These investigators theorized that fluid beds could be accurately described by the application of the fundamental properties of bubbles rising in a fluidized medium. Their work and a recent text by Kunii and Levenspiel [15], presents a comprehensive survey of the present state of knowledge in this area.

The second generation models, in general, represent the fluid bed as a three phase system. The dense phase, is split to include a cloud phase which represents solids directly influenced by rising bubbles. Entrapment of solids in the wakes of rising bubbles is also considered. Information on bubble size and rise velocity, cloud development, gas interchange rates etc., derived from independent investigations, are considered in model development. A representative group of the most noteworthy second generation models, as compiled by Grace [16], are listed in Table I.

The Bubbling Bed Model, developed by Kunii and Levenspiel [21] was shown to be semi-successful in correlating experimental reaction data and is a useful design tool. However, it utilizes an effective or average bubble diameter to describe the bubble phase. This ignores the effect of bubble growth on the operation of the bed and, therefore, seems to be an oversimplification. An improvement can be found in the models of Toor and Calderbank [22], Yates et al [23], and Wen and co-workers [1,24], where changing bubble size is introduced.

TABLE I
SECOND GENERATION FLUIDIZED BED MODELS

ORCUTT et al [17]

HOVMAND and DAVIDSON [18]

PARTRIDGE and ROWE [19]

CHIBA and KOBAYASHI [20]

Wen and Kato [24] investigated reactions using their Bubble Assemblege Model and found the model predicts conversions and concentration profiles reasonably well. This same model in modified form was used by Wen and Yoshida [1] to correlate results of a non-catalytic ore roasting reaction.

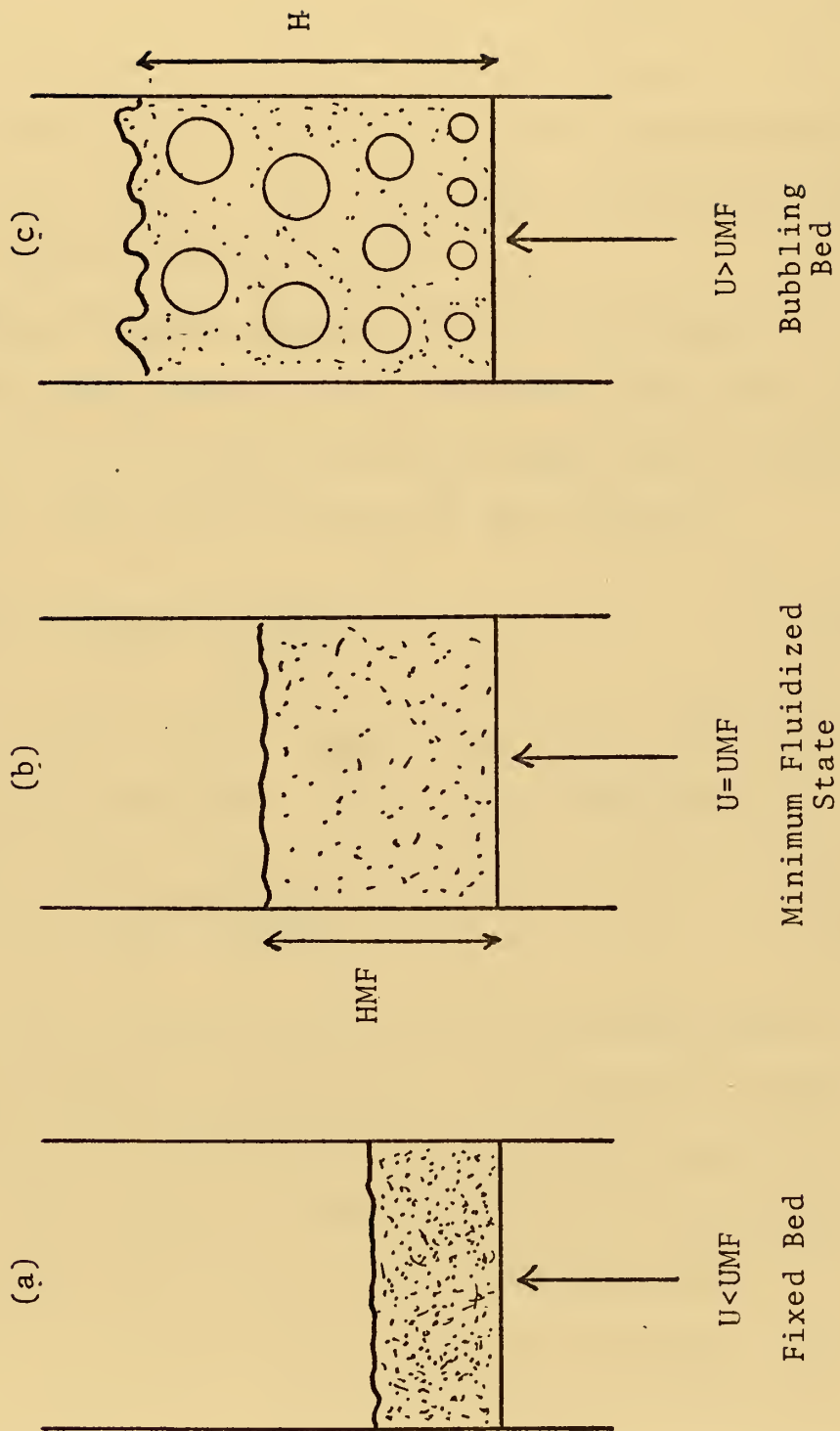
III. MODEL DEVELOPMENT

The first step in the development of a model for a fluidized bed is the study of the qualitative nature of fluidization. In Figure 2, the three possible states of a bed of solids having a gas flowing through it are shown. At low gas flow rates, Figure 2a, the solids are in a fixed bed condition. The gas passes through the interstitial voids of the solids. As the gas flow is increased, a point will be reached where the pressure drop of the gas is sufficient to support the weight of the bed. At this gas flow rate, the bed becomes fluidized and has many of the properties of ordinary liquids. In this state, Figure 2b, the bed is characterized by a minimum fluidization velocity, voidage, and height.

Increasing the gas flow above the minimum fluidization rate causes the bed to transition to a state of vigorous and violent bubbling as shown in Figure 2c. This state is of the greatest importance for it represents the condition of most industrial fluid bed reactors.

In modeling the bubbling fluidized bed, two assumptions are universally accepted; 1) isothermal operation and 2) the flow through the bubble phase represents all gas flow above that required for the minimum fluidization, i.e., $(U - U_{MF})$. These assumptions were used in the model developed in this investigation. This model represents a modified form of the Bubble Assemblege Model proposed by Wen and Yoshida [1].

Figure 2. States of the Gas-solid System.



A. OVERALL BED MODEL

The fluidized bed was divided into a number of backmixed reactors connected in series as shown in Figure 3. The height of each section corresponds to the average bubble diameter at that level. The model thus accounts for changing bubble diameter within the bed.

1. Bubble Size and Section Height Calculation

The bubble diameter was calculated using the relation of Kobayashi [25] who found that experimental data on bubble sizes could be correlated by the equation

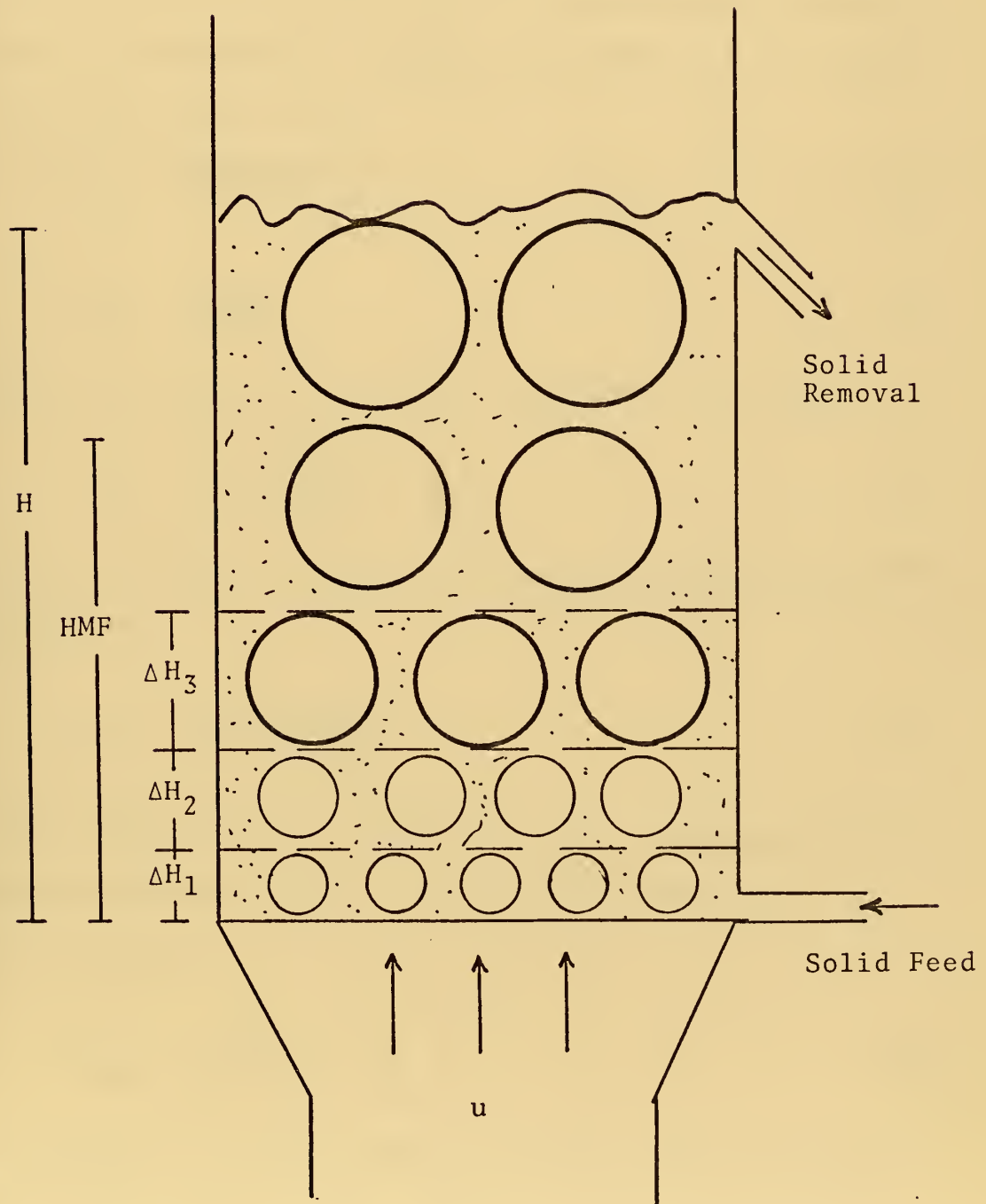
$$DB = 0.684 \rho p D_p \left(\frac{U_o}{UMF_o} \right) \quad (3)$$

To account for the initial bubble size at the surface of the distributor Kobayashi's relation was modified to

$$DB = 0.684 \rho p D_p \left(\frac{U_o}{UMF_o} \right) + D_o \quad (4)$$

where D_o is the initial bubble size at the distributor plate. This quantity is difficult to estimate for beds having porous plate distributors and therefore must be estimated. For perforated plate distributors, however, D_o can be estimated based on the work of Davidson and Harrison [14]. It was shown by these investigators that the bubbles produced in fluidized beds have essentially the same properties as bubbles produced in ordinary liquids having a small viscosity. On this basis D_o can be calculated from the equation developed for predicting the

Figure 3. Sectionalized Model of the Fluid Bed Reactor.



diameter of bubbles produced in ordinary liquids at a single orifice

$$D_o = \left(\frac{6}{\pi} \right)^4 \left(\frac{U - U_{MF}}{N_o} \right)^4 g^{1/2} \quad (5)$$

The averaging procedure used in calculating the individual section heights is graphically depicted in Figure 4. For the first section

$$\Delta H_1 = \frac{D_o + XM\Delta H_1 + D_o}{2} \quad (6)$$

$$\Delta H_1 = \frac{2D_o}{(2-XM)} \quad (7)$$

Repeating the procedure for the second section yields

$$\Delta H_2 = 2D_o \frac{(2+XM)}{(2-XM)^2} \quad (8)$$

In general, it can be shown the average height of the N^{th} section is

$$\Delta H_N = 2D_o \frac{(2+XM)^{N-1}}{(2-XM)^N} \quad (9)$$

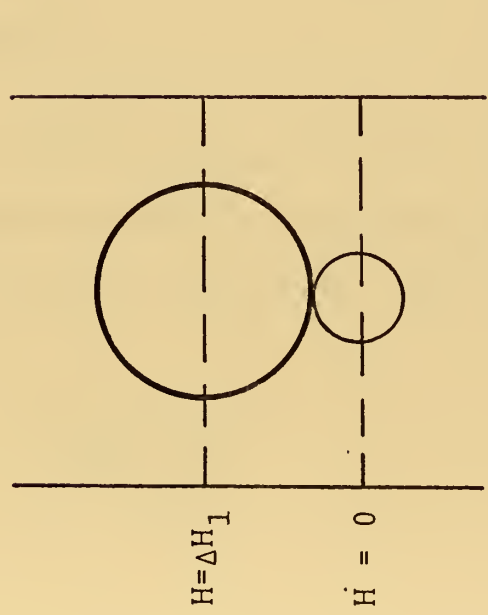
The bubbles were considered to grow continuously until the maximum bubble diameter predicted by Harrison et al [26] is reached

$$D_{B_{MAX}} = \left(\frac{U_T}{0.711} \right)^2 \cdot \frac{1}{g} \quad (10)$$

This maximum is attained when the upward velocity of the bubble equals the terminal velocity of the bed particles.

Figure 4. Averaging Procedure Used to Determine Section Heights.

$$DB_1 = X_M \Delta H_1 + Do$$



The calculation of the terminal velocity is given in the Appendix.

2. Bed Voidage and Height Calculations

The bed conditions at minimum fluidization must be defined prior to the calculation of the operational bed characteristics. These calculations were completed using well defined experimental correlations that are given in the Appendix.

Davidson and Harrison [14] have shown that the rise velocity of a crowd of bubbles in a fluid bed can be calculated from the relation

$$U_{BR} = U - UMF + 0.711 \left(g \frac{DB}{12} \right)^{\frac{1}{2}} \quad (11)$$

It was assumed that the expansion of the bed over that at minimum fluidization is a reflection of the total volume of bubbles in the bed

$$VB_T = (H - HMF) S_T \quad (12)$$

and that an average bubble size can be taken as the bubble size at a height equal to $HMF/2$. The bed expansion ratio was calculated by combining equations (4), (11), and (12) to give

$$\frac{H - HMF}{H} = \frac{(U - UMF)}{0.711 \left(\frac{g DB_{avg}}{12} \right)^{\frac{1}{2}}} \quad (13)$$

where

$$DB_{avg} = XM \left(\frac{HMF}{2} \right) + Do \quad (14)$$

This equation was tested by Wen and Yoshida [1] and shown to correlate experimental bed heights to within 10%.

Based on the above result, the bed voidage was calculated as

$$1 - \epsilon = \frac{HMF}{H} (1 - \epsilon_{MF}) \quad (15)$$

B. SECTION MODEL

The sections into which the bed was divided were treated as having three phases; a bubble phase, a cloud and wake phase and an emulsion phase. Figure 5 shows a single bubble and the three phases. Flow within each phase was assumed to be completely backmixed. This implies uniform gas concentrations and uniform reactant conversion levels within each phase.

1. Bubble Phase Description

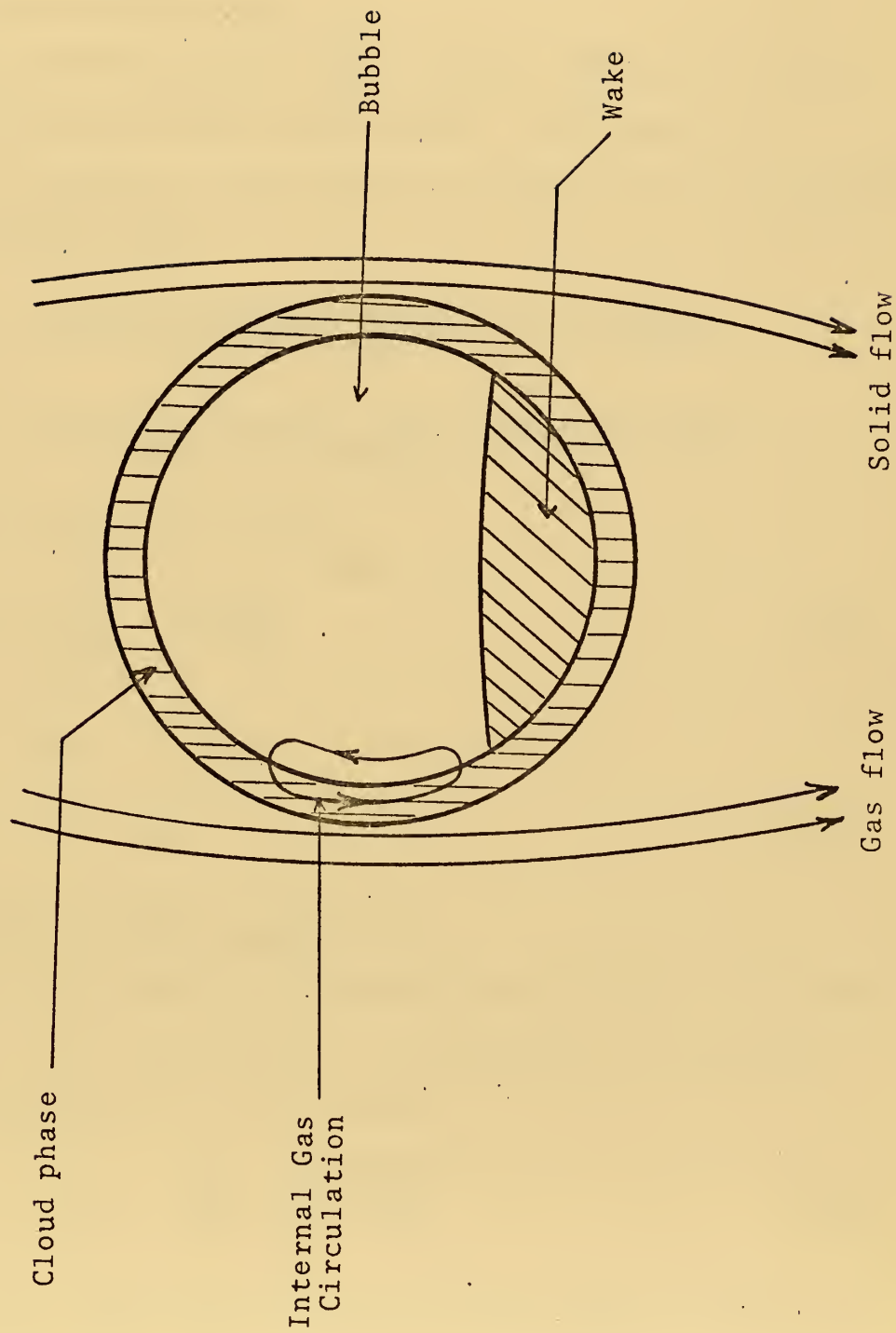
The equations used to describe the bubble phase are based on experimental results which indicate a bubbling fluidized bed can be treated as analogous to a bubbling inviscid liquid.

The relative rise velocity of a single bubble was calculated from the Davies-Taylor [27] equation

$$U_{BREL} = 0.711 \left(g \frac{DB}{12} \right)^{\frac{1}{2}} \quad (16)$$

The relative rise velocity is the rise velocity of a bubble through a bed at minimum fluidization conditions. In a vigorously bubbling bed, the section of the bed ahead of the bubble moves upward with a velocity equal to U_{UMF} .

Figure 5. Bubble Representation.



The absolute rise velocity of the bed then becomes

$$U_{BR} = U - UMF + U_{BREL} \quad (17)$$

This equation was proposed by Nicklin [28] and later by Davidson and Harrison [14].

An accurate model of any section must predict the number of bubbles within that section. The number of bubbles was predicted from the bed expansion ratio according to the following logic

$$N = \frac{\text{Volume of Section Comprised of Bubbles}}{\text{Volume Per Bubble}}$$

$$N = \frac{\text{Volume of Section} \times \text{Bed Expansion Ratio}}{\text{Volume Per Bubble}}$$

This yields upon substitution

$$N = \frac{6 S_T}{\pi \Delta H_N^2} \cdot \frac{\epsilon - \epsilon_{MF}}{1 - \epsilon_{MF}} \quad (18)$$

The total volume of bubbles is then given by

$$VB = N \cdot \frac{\pi}{6} DB^3 \quad (19)$$

2. Cloud and Wake Description

The cloud phase was described according to the model of Davidson [29] which permits calculation of the cloud diameter according to the relation

$$DC^3 = DB^3 \cdot \frac{U_{BREL} + 2UMF/\epsilon_{MF}}{U_{BREL} - UMF/\epsilon_{MF}} \quad (20)$$

On this basis, the total volume of cloud phase in each section becomes

$$VC = VB \cdot \frac{3UMF/\varepsilon_{MF}}{U_{BREL} - UMF/\varepsilon_{MF}} \quad (21)$$

The cloud was assumed to have a voidage equal to the bed at minimum fluidization.

The wake was described using the results of Rowe and Partridge [30]. These investigators have shown that the wake comprises approximately thirty percent of the bubble volume. A plot of their results is given in the Appendix and was used to estimate the parameter Alpha which equals the ratio of the wake to bubble volume. The wake was also assumed to have a voidage equal to the bed at minimum fluidization.

3. Emulsion Description

The emulsion phase includes all of the remaining section volume

$$VE = \Delta H \cdot S_T - VC - VB \quad (22)$$

having a voidage equal to the bed at minimum fluidization. It was assumed in this investigation that for operating conditions where U/UMF is large that the velocity of the gas through the emulsion phase is zero. This assumption finds substantiation in the work of Latham et al [31] and Kunii and Levenspiel [15]. These investigators found that the emulsion gas will reverse its direction ($U_e=0$) when $U/UMF > 2.7 \approx 6.0$.

4. Solid Movement and Gas Exchange

The primary mechanism of solid circulation within the bed is by transport in the wakes of bubbles. The solid

is entrained by rising bubbles and carried upward with a velocity equal to the rise velocity of the bubbles. During the bubble's movement through the bed, the solids in its wake are continuously exchanged with the bulk emulsion solids. In this investigation, the exchange coefficient for the solids was assumed to be infinite.

Solids in the bulk emulsion phase move downward with the same volumetric flow rate as solids carried upward in the wakes. As a result, there is no net flow of solids across any horizontal plane within the bed.

For a system in which a solid is continuously fed to the bottom of the bed and removed from the top, a net upward flow does exist and is equal to the volumetric flow rate of the feed. Mathematically, this model can be expressed as

$$WB_N = \frac{W_f}{S_T} \cdot S_{BN} + \frac{\alpha S_{BN} U_{BRN}}{144.0} \quad (23)$$

$$WE_{N+1} = \frac{\alpha S_{BN} U_{BRN}}{144.0} - \frac{W_f}{S_T} \cdot (S_T - S_{BN}) \quad (24)$$

where $WB(N)$ represents solids flowing upward to the $(N+1)^{th}$ section from the N^{th} section and $WE(N+1)$ represents solids flowing downward into the N^{th} section from the $(N+1)^{th}$ section.

The overall gas exchange coefficient was calculated using the correlation of Kobayashi et al [32]. Based on a unit volume of bubbles, this expression can be expressed as

$$K_{be} = \frac{4.331}{DB} \quad (25)$$

C. KINETICS

Non-catalytic gas-solid reactions in which the reacting particles do not change size were studied in this model. Examples of this type of reaction include sulfide ore roasting, reduction of iron ore, and calcination of limestone. The following stoichiometric equation was used to represent these reactions



For this stoichiometric relation, the first order irreversible reaction rate equation can be written as

$$-\frac{1}{A_{rx}} \frac{dN_a}{dt} = -\frac{1}{bA_{rx}} \frac{dN_b}{dt} = k_c \overline{C_g} \quad (27)$$

The reaction was assumed to proceed according to the shrinking core reaction model [1,33]. This model assumes the reaction begins as the surface of the material and proceeds inward; the reaction zone being the surface of the constantly shrinking unreacted core. The particle maintains its structural integrity as a result of the formation of a completely converted inert ash which surrounds the unreacted core. A time history of the reacting particle is shown in Figure 6. It was also assumed that the overall conversion rate is controlled by the chemical reaction step. This implies that the diffusion of gaseous reactant occurs much faster than the reaction at the surface of the core and, therefore, a gas concentration gradient between the bulk gas phase and the core surface does not exist.

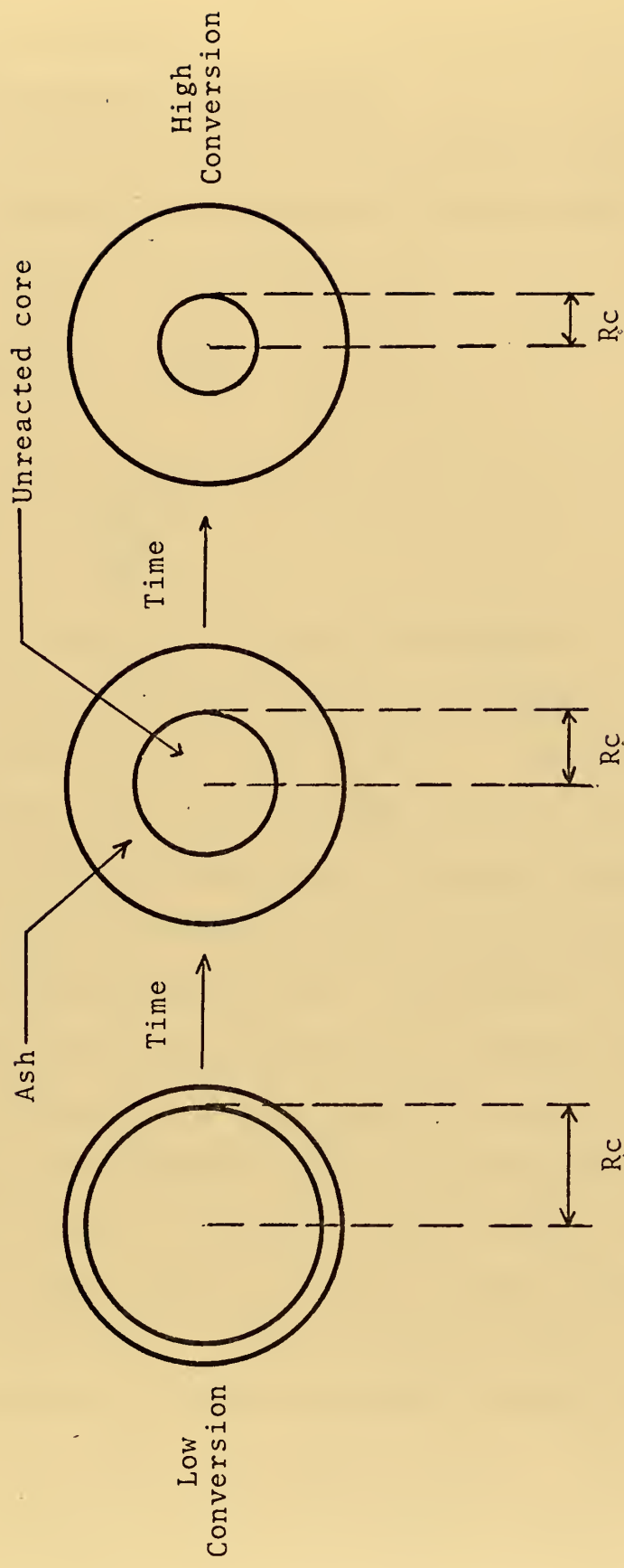


Figure 6. Shrinking Core Reaction Model.

D. MATERIAL BALANCE

1. Preliminary Assumptions

A modified reaction rate constant based on unit volume of solids was defined by dividing both sides of Equation (27) by V_o to give

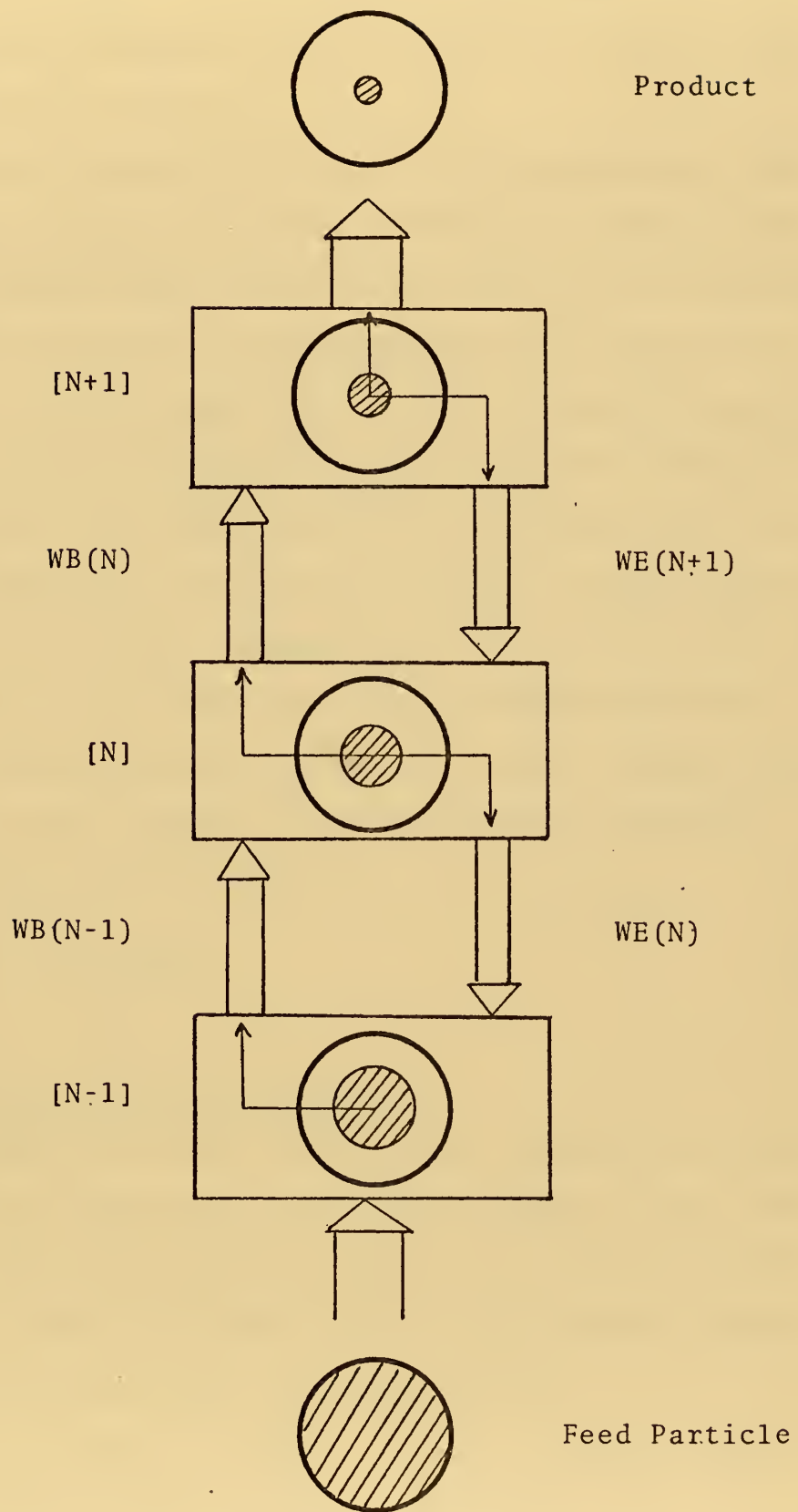
$$-\frac{1}{V_o} \frac{dN_A}{dt} = Kr \overline{Cg} \quad (28)$$

where

$$Kr = \frac{24k_c R_c^2}{D_p^3} \quad (29)$$

Kr is not a constant at a given temperature. It depends upon the core radius, R_c , which is a measure of the average level of conversion of the solids. It was assumed in this investigation that each of the N sections into which the bed was divided contains solids having a uniform conversion level or stated in terms of the shrinking core model having an equal unreacted core size. Furthermore, because of backmixing within each section, the solids swept upward from the N^{th} section to the $(N+1)^{th}$ section in the wake of bubbles were assumed to have a conversion level characteristic of the N^{th} section. This is also true for the downward flowing emulsion solids. These assumptions are shown in Figure 7. It should be noted that no real physical significance can be attached to the concept of having an average core radius within each section. It is obvious that the radius of the solids entering the N^{th} section from the $(N+1)^{th}$ section does not increase to that of the material

Figure 7. Core Size Distribution.



in the N^{th} section. This assumption was made merely to simplify the mathematical representation in terms of the section material balances.

To further simplify the physical representation, the shrinking core model was used to define an average solid reactant concentration for any particular solid conversion level. This approach can be explained with the aide of Figure 8. It was assumed that within each particle, reactant is uniformly dispersed through the entire volume of the particle. Since the shrinking core model states that reaction takes place only at the surface of the unreacted core, using the above assumption it can be stated that the unreacted core of a partially converted particle has a reactant concentration equal to the initial reactant concentration. The average concentration for the entire particle was then estimated as

$$CS = \frac{CS_o V_{\text{core}}}{V_o} \quad (30)$$

2. Section Material Balances

Steady state mass balances on the gaseous reactant were used to characterize the flow streams of the system. Figure 9 shows an individual section and the associated gas flow streams. The material balances for the bubble phase and emulsion phase can be written as

$$\begin{aligned} U_{\text{vol}} [CGB_{N-1} - CGB_N] + (K_{be})_N V_{B_N} [CGE_N - CGB_N] \\ - \gamma_{cN} K_{rN} CGB_N = 0 \end{aligned} \quad (31)$$

Figure 8. Radial Solid Concentration Profile.

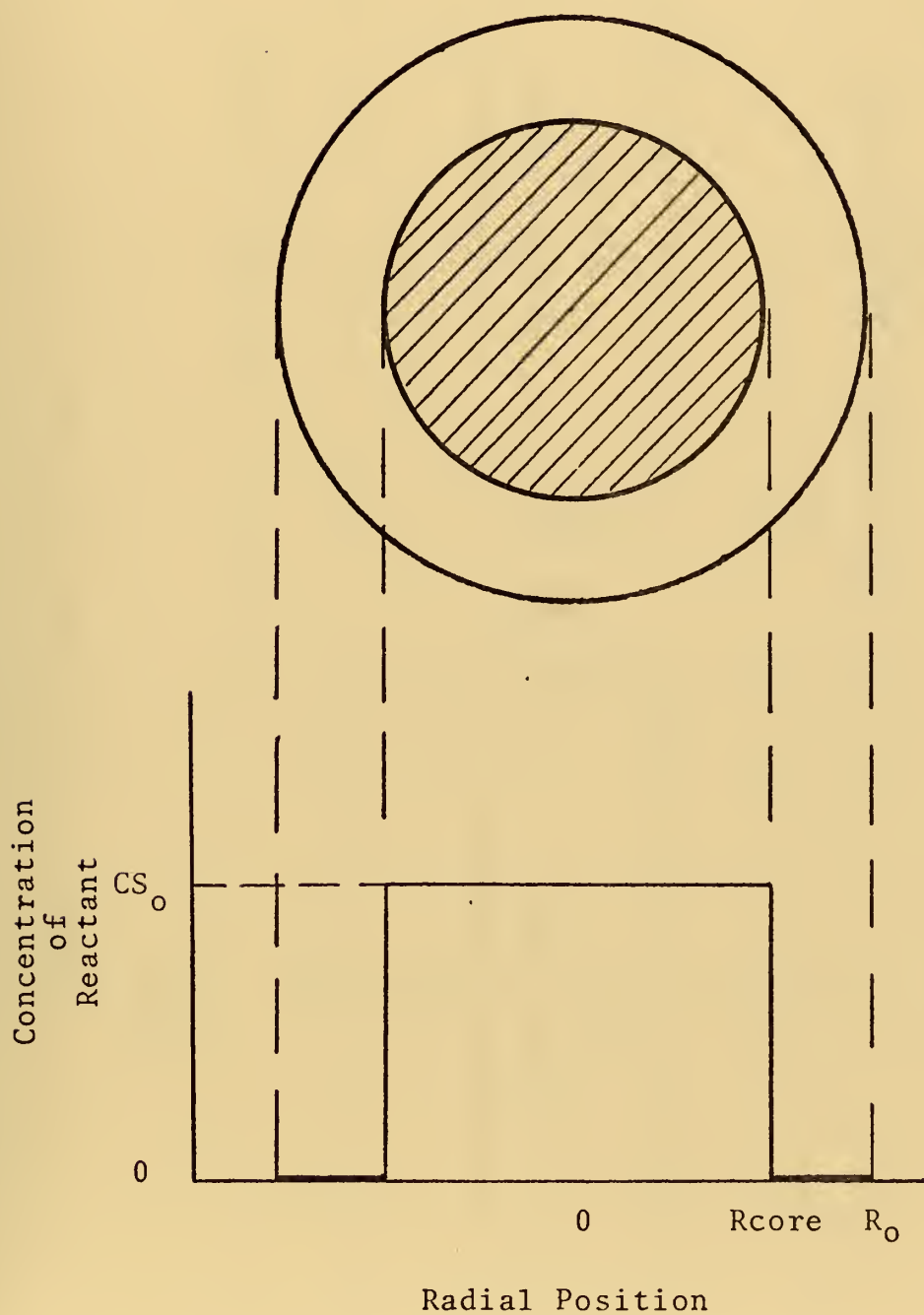
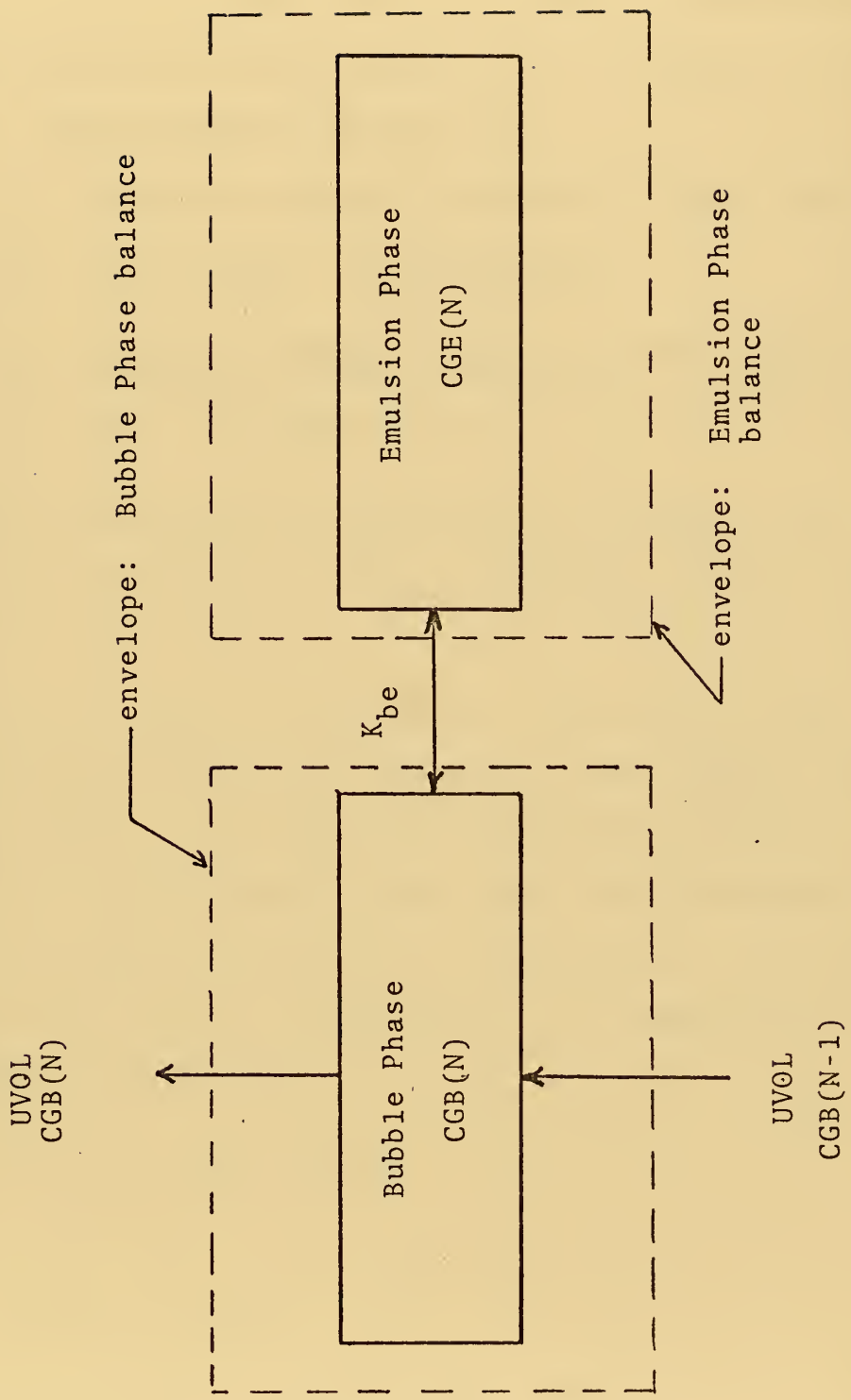


Figure 9. Section Gas Flow Representation.



$$(K_{be})_N [CGB_N - CGE_N] - \gamma_{eN} K_{rn} CGE_N = 0 \quad (32)$$

Included in the reaction term are γ_c and γ_e which define the distribution of solids between the two phases of the section. These terms are defined as

γ_c = Volume of Solids Dispersed in Clouds and Wakes

$$\gamma_c = [VC_N + \alpha VB_N] \cdot [1 - \varepsilon MF]/1728.0 \quad (33)$$

γ_e = Volume of Solids Dispersed in The Emulsion

$$\gamma_e = VE_N \cdot [1 - \varepsilon MF]/1728.0 \quad (34)$$

The material balances were derived on the basis of zero gas flow in the emulsion and complete backmixing within each phase.

In the top reactor section, the cloud phase volume must be modified to account for extension of the bubbles above the bed surface. The bubble was described as shown in Figure 10. In this modification, only the fractional volume of the cloud phase associated with that part of the bubble below the bed surface is considered. The equations for cloud phase then become

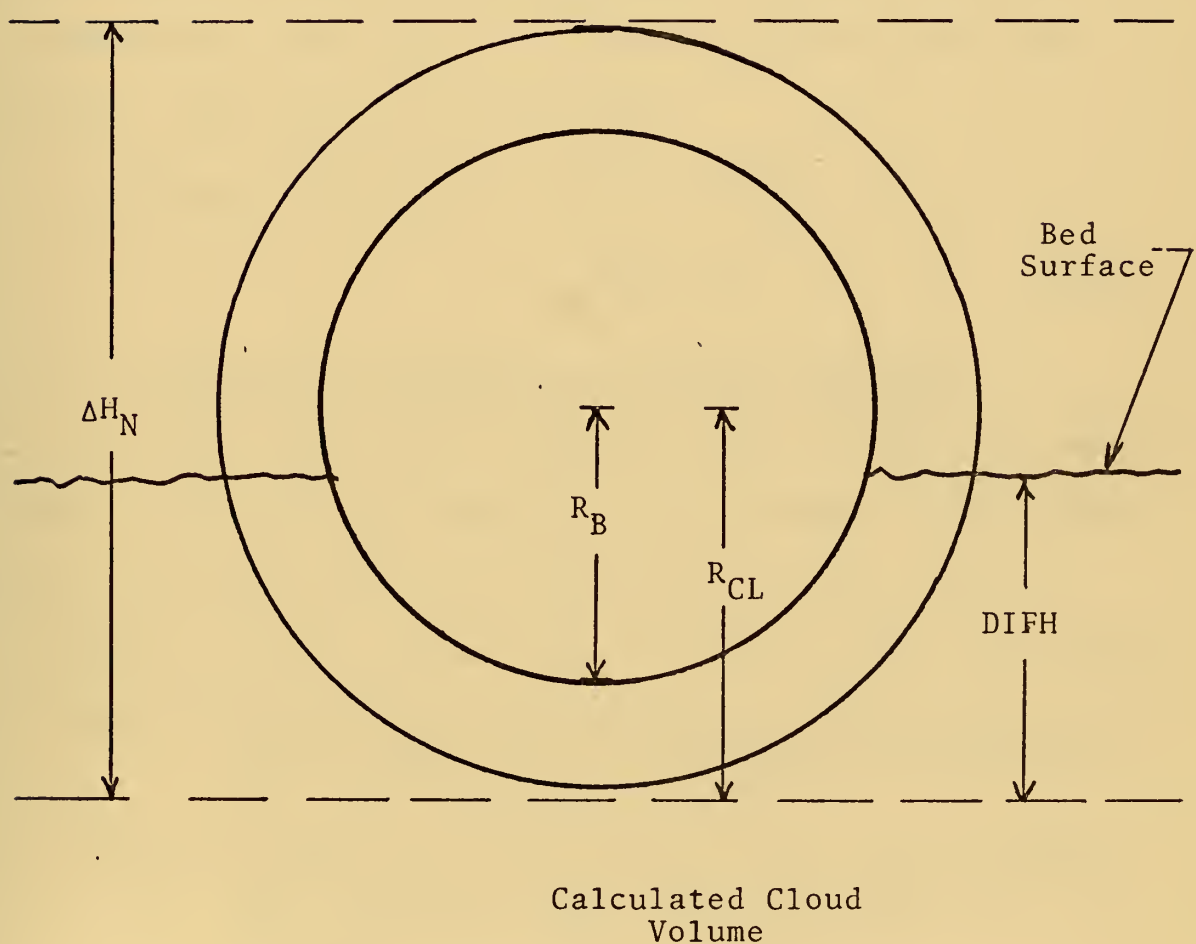
$$VC = N \cdot [V_{FR} - VB_{FR}]$$

where

$$DIFH \leq 0.5 \Delta H_N$$

$$V_{FR} = 1.0472 [DIFH]^2 [3.0 R_{cl} - DIFH] \quad (35)$$

Figure 10. Top Section Modification.



$$VB_{FR} = 1.0472 [DIFH - R_{C\ell} + R_B]^2 [2.0R_B - DIFH + R_{C\ell}] \quad (36)$$

$$DIFH > 0.5 \Delta H_N$$

$$VB_{FR} = V_{T1} - 1.0472 [\Delta H - DIFH]^2 [3.0R_{C\ell} - \Delta H + DIFH] \quad (37)$$

$$VB_{FR} = VB_1 - 1.0472 [\Delta H - DIFH - R_{C\ell} + R_B]^2 [2.0R_B - \Delta H + DIFH + R_{C\ell}] \quad (38)$$

An overall material balance on both the solid and gas streams was derived from Figure 11 which shows the bed representation from the $(N-1)^{th}$ section down to the feed section. An overall balance yields

$$\begin{aligned} bU_{vol} [CG_O - CGB_{N-1}] &= W_f CS_O + WE_N CS_N \\ &\quad - WB_{N-1} CS_{N-1} \end{aligned} \quad (39)$$

3. Solution of the Material Balance Equations

A trial and error procedure was used to obtain solutions to the material balances of the system. The procedure can be characterized by the three major steps involved

Step 1: Assume the exit gas stream concentration $CGB(N)$

Step 2: Solve each of the section material balances to obtain the required initial gas concentration for the assumption of Step 1.

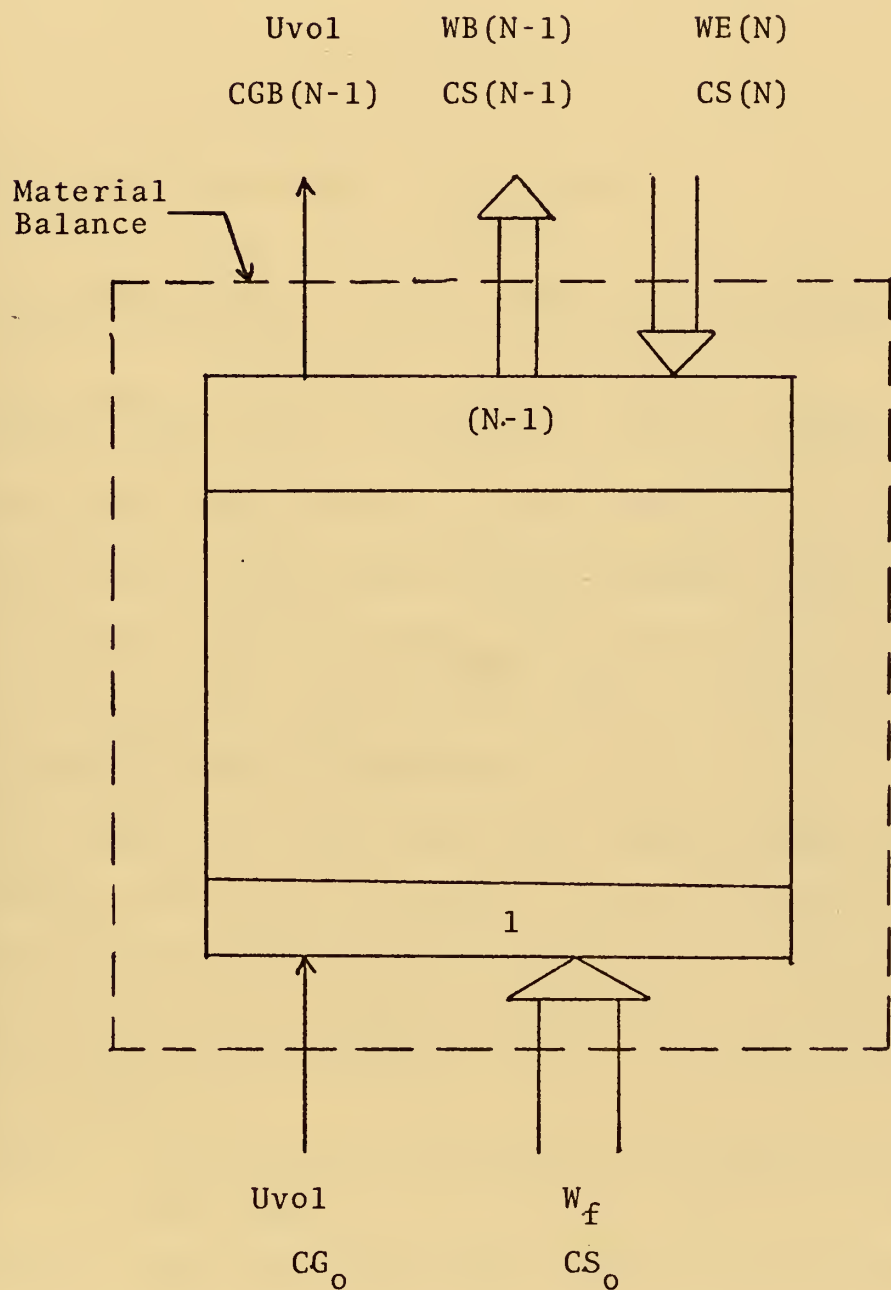
Step 3: Compare the calculated initial gas concentration with the known value (CG_O) and continue the calculation until they are equal by adjusting the value of $CGB(N)$.

A detailed description of the completion of Step 2 is given in the next three sections.

a. Calculation for the Top Section

The bed with the N^{th} section isolated is shown

Figure 11. Flow Streams for Overall Material Balance.



in Figure 12. Four material balances can be derived from this figure:

$$U_{vol} [CGB_{N-1} - CGB_N] + (K_{be})_N V_{B_N} [CGE_N - CGB_N] \\ - \gamma_{cN} K_{rN} CGB_N = 0 \quad (40)$$

$$(K_{be})_N V_{B_N} [CGB_N - CGE_N] - \gamma_{eN} K_{rN} CGE_N = 0 \quad (41)$$

$$bU_{vol} [CG_O - CGB_{N-1}] = w_f CS_O + w_E CS_N - w_{B_{N-1}} CS_{N-1} \quad (42)$$

$$bU_{vol} [CGB_{N-1} - CGB_N] = w_{B_{N-1}} CS_{N-1} - w_f CS_N - w_E CS_N \quad (43)$$

Equations (40) and (41) are the gas reactant material balances for the bubble and emulsion phase, Equation (42) is the overall material balance over the $(N-1)^{th}$ section to the feed section, and Equation (43) is the balance for both streams in the N^{th} section.

The solution of these equations requires knowledge of the average core size of material in the N^{th} section for evaluation of K_r , the reaction rate constant. This is not known and therefore a second trial and error solution proceeds as follows.

Step 1: Guess Rcore and calculate Kr from Equation (29) and Vcore.

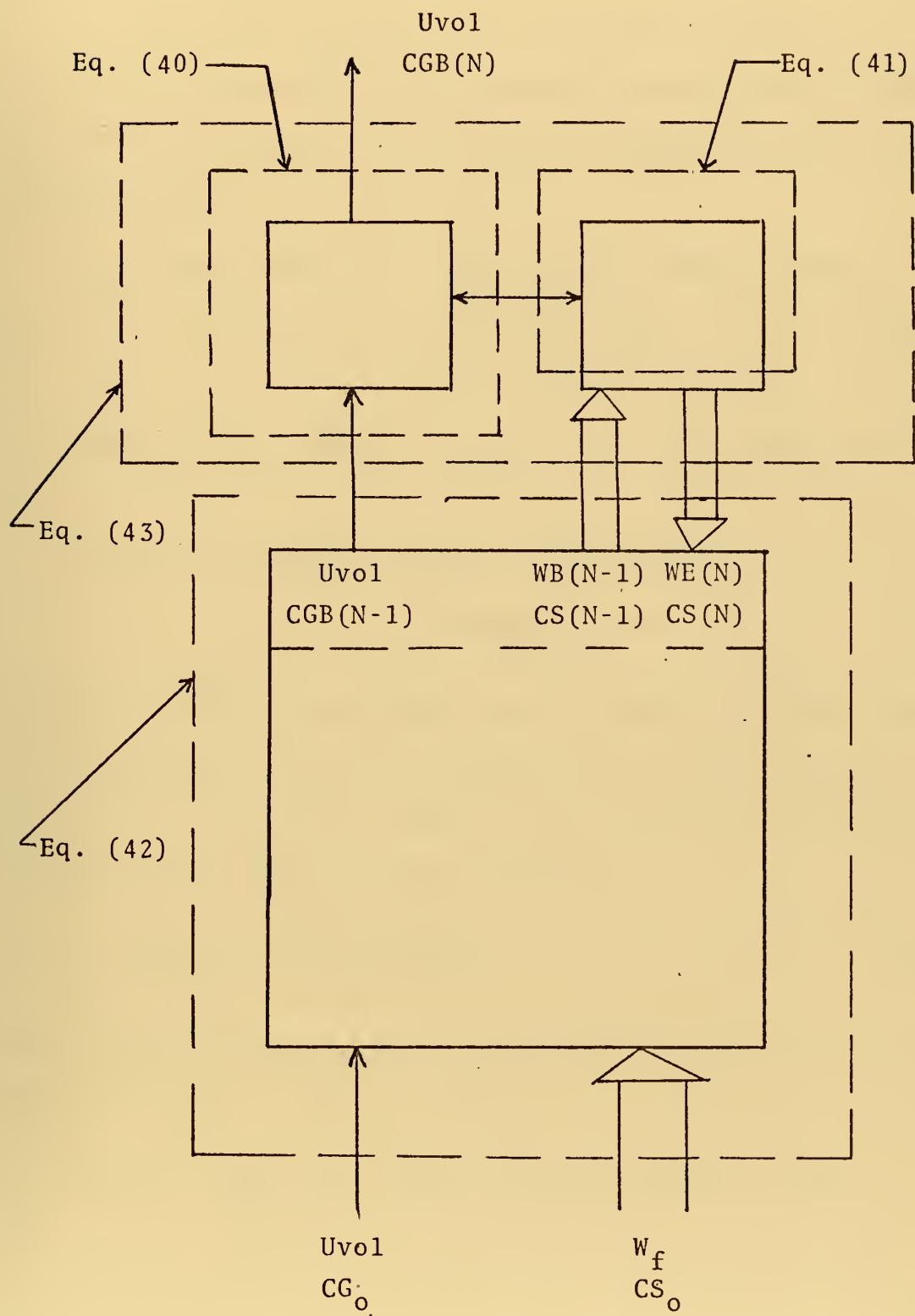
Step 2: Calculate CGE(N) and CGB(N-1) from Equations (41) and (40).

Step 3: Calculate CS(N) from Equation (30).

Step 4: Calculate CS(N-1) from Equation (42).

Step 5: Repeat the calculations until the section material balance Equation (43) is satisfied.

Figure 12. Top Section Material Balances.



When Step 5 has been completed, the solution proceeds to the $(N-1)^{th}$ section.

b. Calculations for the $(N-1)^{th}$ Section

The middle bed sections are characterized by the three standard material balance equations which can be written as

$$U_{vol} [CGB_{N-2} - CGB_{N-1}] + (K_{be})_{N-1} VB_{N-1} [CGE_{N-1} - CGB_{N-1}] - \gamma_{cN-1} Kr_{N-1} CGB_{N-1} = 0 \quad (44)$$

$$(K_{be})_{N-1} VB_{N-1} [CGB_{N-1} - CGE_{N-1}] - \gamma_{eN-1} Kr_{N-1} CGE_{N-1} = 0 \quad (45)$$

$$bU_{vol} [CG_o - CGB_{N-1}] = W_f CS_o + WE_{N-1} CS_{N-1} + WB_{N-2} CS_{N-2} = 0 \quad (46)$$

Solution of these equations does not require a trial and error procedure since the average core size of material in the $(N-1)^{th}$ section is fixed by the results of the calculations on the $(N)^{th}$ section through

$$CS_{N-1} = \frac{CS_o V_{core}_{N-1}}{V_Q} \quad (47)$$

This equation defines Rcore and Kr for the $(N-1)^{th}$ section. Solution then proceeds as follows

Step 5: $CGE(N-1)$, $CGB(N-2)$ are calculated from Equations (45) and (44).

Step 6: $CS(N-2)$ is calculated from Equation (46).

This procedure is repeated until the feed section is reached.

c. Calculation for the Feed Section

The material balances around the feed section can be written as

$$U_{vol} [CG_o - CGB_1] + (K_{be})_1 V B_1 [CGE_1 - CGB_1] - \gamma_{c1} K r_1 CGB_1 = 0 \quad (48)$$

$$(K_{be})_1 V B_1 [CGB_1 - CGE_1] - \gamma_{e1} K r_1 CGE_1 = 0 \quad (49)$$

As is the case for the middle sections, a trial and error procedure is not required for their solution on this basis, solution was completed as follows

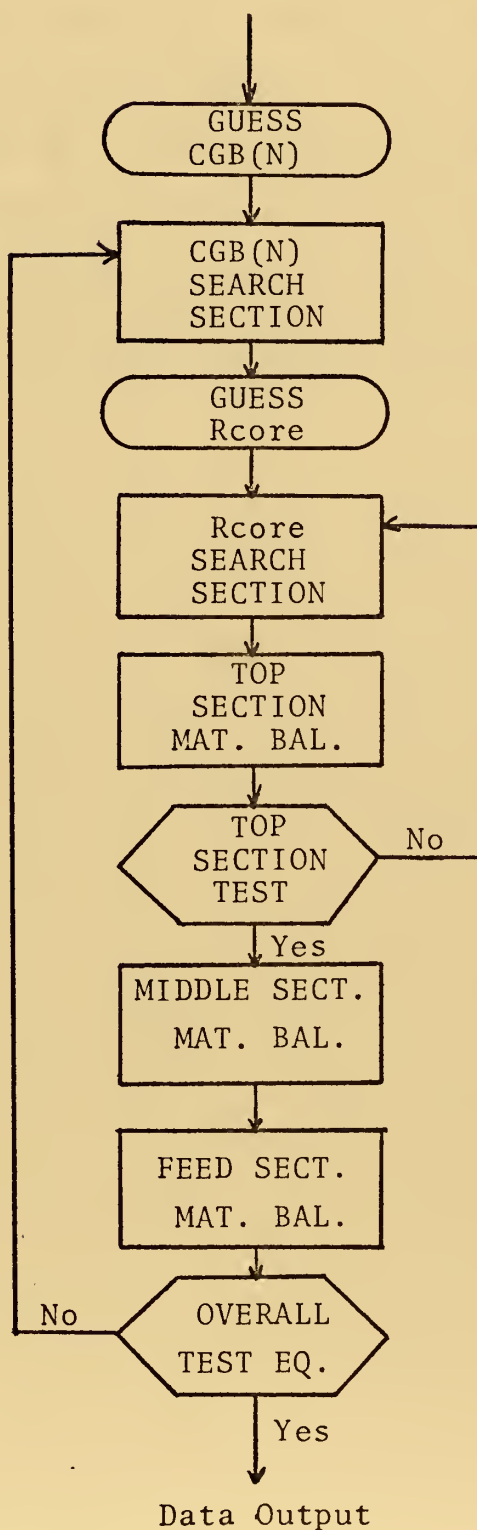
Step 7: Rcore is calculated from CS(1) obtained from the calculations on section two.

Step 8: Kr and CGE(1) are calculated from Equations (29) and (49).

Step 9: CG_o is calculated from Equation (48).

The initial gas concentration calculated in Step 9 is then compared with the known value of CG_o. This provides a test of the validity of the assumed value of the exit gas concentration CGB(N). If the calculated CG_o does not equal the experimental value, CGB(N) is adjusted and the entire calculation repeated. When the equality exists, the material balances for each section and the overall material balance for the bed have been satisfied and the solution completed. The computer flow chart for the solution of the material balances is given in Figure 13.

Figure 13. Flow Chart for the Solution
of the Material Balances.



E. THE COMPUTER MODEL

The program developed to model the fluid bed reactor is given in the COMPUTER PROGRAM SECTION. The program was designed to be completely self-contained, that is, no external calculations are required. The input variables are listed in Table II. They represent common design variables and therefore would normally be well defined. In Table III the program is divided into its three major sections and the calculations completed in each are listed.

TABLE II
COMPUTER INPUT VARIABLES

-
1. Reactor Diameter
 2. Number of Holes per in.² in the Distributor (0 for Porous Plate)
 3. Weight of Solids in the Bed
 4. Diameter of the Bed Solids
 5. Radius of Reactant
 6. Density of Bed Solids
 7. Density of Reactant
 8. Bed Temperature
 9. Stoichiometric Constant
 10. Kinetic Rate Constant
 12. Molecular Weight of Solid Reactant
 13. Solid Feed Rate
 14. Initial Solid Concentration
 15. Initial Gas Concentration
 16. Superficial Gas Velocity at Room Temperature
 17. Superficial Gas Velocity at the Bed Temperature
 18. Alpha (Volume of Wake/Volume Bubble)
 19. Initial Section Height
 20. Initial Guess of CGB(N)
 21. Increment of Gas Search
-

TABLE III
MAJOR COMPUTER PROGRAM SECTIONS

A. PRELIMINARY CALCULATIONS	B. SECTION CALCULATION	C. MATERIAL BALANCE
1. Gas Properties	1. Bed Voidage	1. Section Gas and Solid Concentrations
2. Bed Characteristics at Minimum Fluidization	2. Section Heights	2. Overall Reactant Conversion
	3. Phase Volumes	
3. Terminal Velocity	4. Solid Distribution Functions	3. Conversion Based on Backmixed Equations
4. Maximum Bubble Size		
5. Average Bubble Size and Bed Height	5. Bubble Rise Velocities	
	6. Gas Exchange Coefficients	
		7. Solid Flow Streams

IV. PRESENTATION AND DISCUSSION OF RESULTS

The model developed in the previous section was used to study a sulfide ore roasting reaction following the stoichiometric equation



The experimental results obtained by Yagi et al [34] were used for evaluating the model. The performance of the model was judged by its ability to predict experimental conversions. This presentation is divided into two sections. In the first, the overall results are presented predicted by the model of Wen and Yoshida [1]. In the second section, the effects of the major assumptions used in the development of the model are investigated. This section represents a detailed study of the model performance.

A. OVERALL RESULTS: GENERAL MODEL PERFORMANCE

In Table IV, the experimental data of Yagi et al [34], the calculated conversions obtained by Wen and Yoshida [1], and those from the model developed in this investigation are tabulated. In these runs, the height of the first section ΔH_1 was assumed to be 1.0 cm. This assumption was proposed by Wen and Yoshida for reactors having porous plate distributors. The validity of this assumption is discussed in another part of this section. The input data for these runs are given in Table VIII of the Appendix.

TABLE IV
COMPARISON OF OVERALL RESULTS WITH LITERATURE DATA

Run No.	Conv. Exp.	Conv. Model	% Error	Conv. WEN	% Error
1	99.4	99.9	0.59	99.8	0.43
2	97.2	99.9	2.77	98.5	1.34
3	88.7	99.4	10.75	90.0	1.47
4	91.0	99.2	8.31	93.0	2.18
6	86.5	97.2	11.05	86.9	0.46
7	93.5	99.7	6.22	95.0	1.61
10	85.4	97.1	12.01	-	-
11	80.6	91.2	11.62	-	-
12	72.4	81.8	11.49	-	-
13	91.7	99.9	8.17	-	-

The data shows that the model predicts conversions which are significantly higher than the experimental values. For experimental runs having relatively high conversions (>90%), the material is essentially completely reacted within the bed (>99% conversion). The average percent error of the calculated conversions for all runs was 8.3%. The maximum error was 12.01% for Run 10 and the minimum was 0.59% in Run 1. The model did not predict for any of the runs, a conversion less than the experimental value. Low percentage error for runs having higher conversion can therefore be expected.

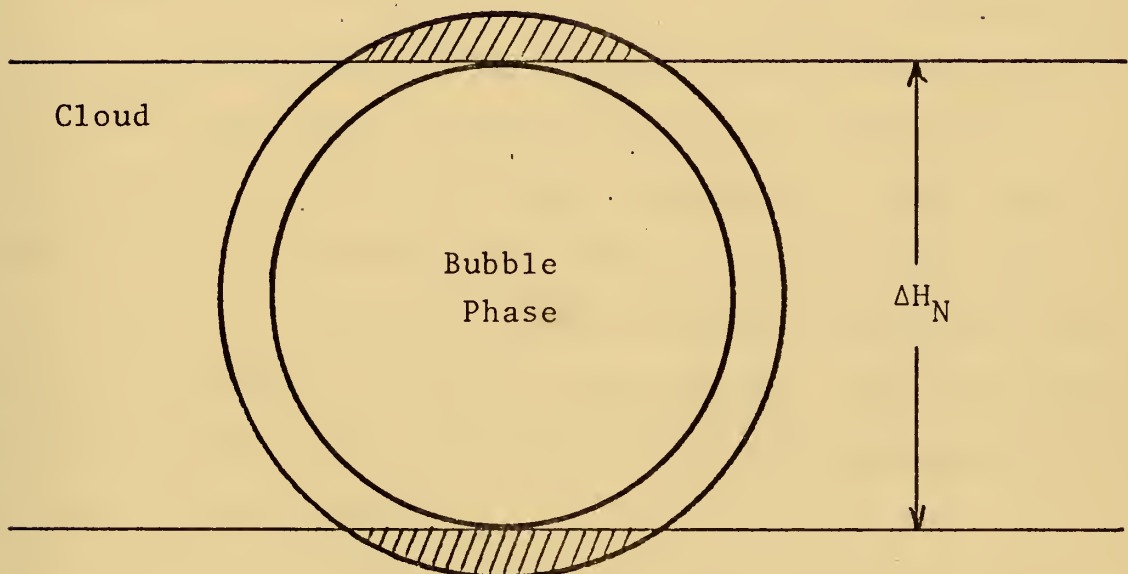
The calculated conversions reported by Wen and Yoshida show much better agreement with the experimental data. The average percentage error for their runs was 1.25%. These investigators did not report results for experimental runs in which low conversions were found and for which the model proposed in this investigation had the highest error. On the basis of the six runs reported by Wen and Yoshida, the error for the proposed model becomes 6.60% .

B. EFFECTS OF THE MAJOR ASSUMPTIONS

1. Modified Section Height Calculation

The height of each section was originally calculated by taking the average bubble diameter at a particular height as described in the MODEL DEVELOPMENT SECTION. When this is done, a portion of the cloud surrounding the bubble actually extends beyond the section boundaries as shown in Figure 14. The volume of the cloud phase associated with

Figure 14. Section Height Based on Bubble Size.



Hatch areas show volume of cloud phase which extends above and below section boundaries

each section, therefore, is slightly larger than the correct value. Furthermore, this portion of cloud volume is counted twice when succeeding sections are considered.

Figure 15 shows a plot of the gas concentrations for the bubble and emulsion phase as a function of height above the distributor. It can be seen that the bubble gas concentration is considerably greater than the concentration of gas in the emulsion phase. As a result, solids in the bubble wake and cloud react with gas of higher concentration than emulsion solids. It was theorized that the inaccuracies in the prediction of the volume of the cloud phase resulting from the section height calculation, might contribute to the prediction of a larger overall conversion.

To test this theory, the section height calculation was modified to include the entire cloud volume. The equations necessary to make this modification and their derivation are given in the Appendix.

The conversion results obtained from the modified program are given in Table V. No significant change in the predicted conversions was found. The overall percent error was 8.30% which equals that found for the original program. The average error for the six runs reported by Wen and Yoshida was found to be only slightly higher at 6.64%. The maximum change in predicted conversion occurred for Run 12 where the conversion calculated from the modified program was found to be 1.6% higher than the original calculation. These results show that the error in cloud phase volume

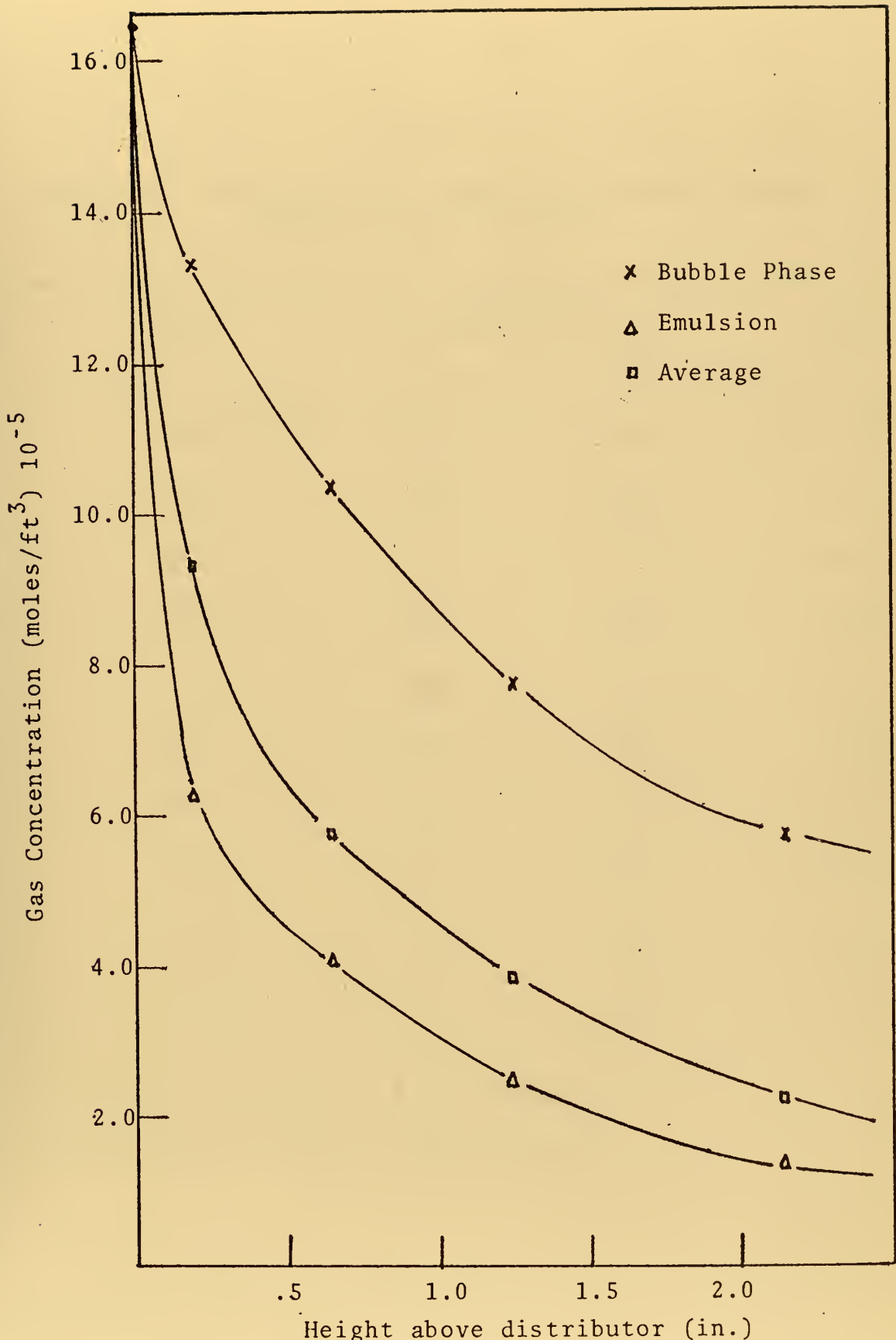


Figure 15. Gas Concentration Profiles for Run 12;
 ΔH_1 Based on Cloud Size.

TABLE V
PREDICTED CONVERSIONS FOR MODEL WITH SECTION HEIGHT
BASED ON THE CLOUD DATA

Run No.	Conv. Exp.	Conversion		% Error B
		A	B	
1	99.4	99.9	99.9	0.59
2	97.2	99.9	99.9	2.77
3	88.7	99.4	99.4	10.73
4	91.0	99.2	99.3	8.36
6	86.5	97.2	97.6	11.10
7	93.5	99.7	99.7	6.24
10	85.4	97.1	97.2	12.15
11	80.6	91.2	91.9	12.29
12	72.4	81.8	83.1	10.67
13	91.7	99.9	99.8	8.17

A: Section Height Based on Bubble Diameter

B: Section Height Based on Cloud Diameter

resulting from calculating the section heights on the basis of average bubble size is not a significant factor. In the rest of this study, however, the modified section height calculation was retained.

2. Backmixing Considerations

In the development of this model, it was assumed that the solids within a particular section have an equal average concentration and conversion level. This concept implicitly assumes that every particle fed to the reactor has a residence time which is equal to that of any other particle. The mean residence time being defined as

$$\bar{t} = \frac{W_t}{\rho p W_f} \quad (51)$$

Investigators [15,35] studying the flow patterns and residence times in fluidized beds have shown that a residence time distribution (RTD) actually exists for the feed particles. This concept implies that some feed solids have a residence time which is far less than the average, while others have residence times greater than the average. As a result, the product of a reaction occurring in a fluidized bed does not have a uniform conversion level. Kunii and Levenspiel [15] proposed that the RTD can be expressed by defining an exit age distribution function $E(t)$ as

$$E(t) = \frac{1}{\bar{t}} e^{-t/\bar{t}} \quad (52)$$

where $E(t)dt$ is the fraction of solids staying in the bed for a time between t and $t+dt$. This expression has been

shown to correlate experimental residence times very accurately.

The normalized exit age distribution function is plotted in Figure 16. The shaded area represents the fraction of material having a residence time equal to $\bar{t} \pm 10\%$. This fraction was found to be only 7.2% of the total bed material. This observation indicates that the assumption that all the solids in the bed have a residence time equal to \bar{t} might be a gross oversimplification leading to poor calculated results.

To test this theory, overall bed conversions based on a non-uniform bed residence time were calculated using average gas concentrations predicted by the model. The equations used were those given by Kunii and Levenspiel [15]. According to these authors, the mean conversion of the product stream can be defined as

$$X_B = 3\left(\frac{\bar{t}}{\tau}\right) - 6\left(\frac{\bar{t}}{\tau}\right)^2 + 6\left(\frac{\bar{t}}{\tau}\right)^3 \left(1.0 - e^{-\tau/\bar{t}}\right) \quad (53)$$

where the time for complete conversion is equal to

$$\tau = \frac{\rho' p D_p}{2 b k c \bar{C}_g} \quad (54)$$

The overall average gas concentration \bar{C}_g was calculated as a weighted average of the section gas concentrations.

$$\bar{C}_g = \frac{\sum_{N=1}^N \bar{t}_N \bar{C}_g_N}{\bar{t}} \quad (55)$$

The results of the calculation are presented in Table VI.

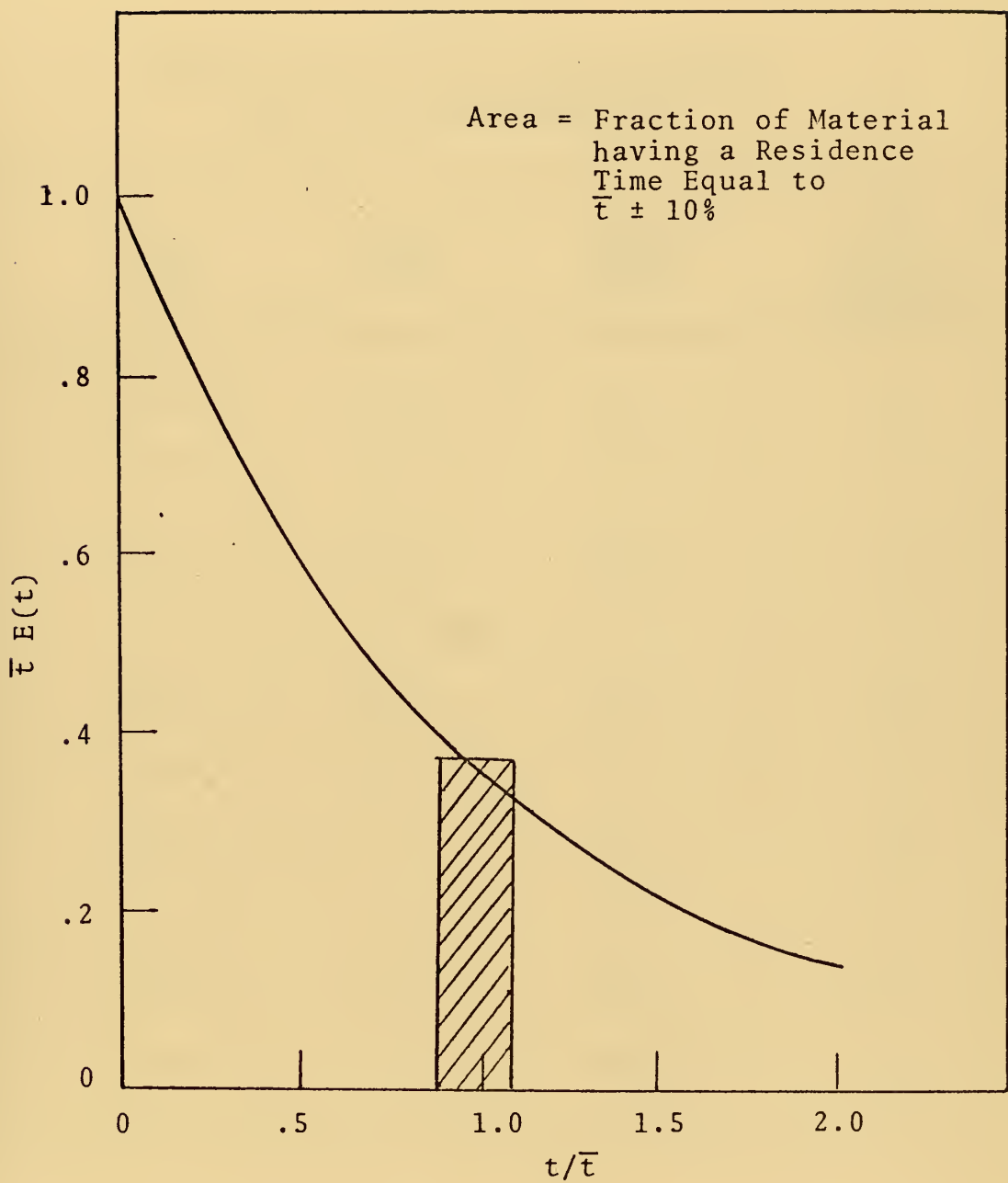


Figure 16. Exit Age Distribution.

TABLE VI
RESULTS OF CONVERSION CALCULATIONS
FROM BACKMIXED EQUATIONS

Run No.	Conv. Exp.	Conv. WEN	Conv. Model B.M.	% Error for B.M. Convers.
1	99.4	99.8	99.5	0.1
2	97.2	98.5	98.9	1.75
3	88.7	90.0	95.6	7.78
4	91.0	93.0	94.9	4.29
6	86.5	86.9	87.8	1.60
7	93.5	95.0	97.1	3.85
10	85.4	-	87.9	2.93
11	80.6	-	75.7	6.08
12	72.4	-	61.2	15.47
13	91.7	-	98.2	7.09

The conversions calculated from the backmixed equations show considerably better agreement with experimental results. The overall average error was reduced to 5.08% and the error for the first six runs to 3.21%. These compare with errors of 8.30% and 6.64% obtained from the model. These results indicate that neglecting the existence of a residence time distribution for the bed particles causes the prediction of conversions which are high when compared with experimental results.

The Bubble Assemblage Model proposed by Wen and Yoshida does account for the non-uniform residence times of the bed particles. The close agreement of their results with experimental data is a further indication that the assumption of uniform solid conversion levels in each section incorporated in the model proposed in this investigation is an oversimplification.

3. Analysis of the Initial Reactor Section

One of the major assumptions required in the analysis of the model performance was the assumption that the height of the first section is equal to 1.0 cm. This assumption is necessary because the reactor used by Yagi had a porous plate distributor for which an accurate calculation of initial bubble size is not possible. The effects of this assumption on their model's performance were tested by Wen and Yoshida. They concluded that the calculated conversions were not sensitive to the height of the first section. Gas and solid reactant concentration profiles given by these investigators, however, show very large changes occurring in the area

directly above the distributor. This observation indicates that the conclusion that the initial section height does not effect the overall results might not be adequate for all reaction conditions. In this section, the results of a detailed study of the first reactor section are given.

It was found that essentially all the reaction occurs in the first section of the bed. Data supporting this observation are given in Table VII. These data show that the concentration of solids leaving the first section is reduced to very nearly the final product concentration level. This observation is not surprising. Many investigators [36,37] have reported that the primary reaction zone is the area directly above the distributor. This fact emphasizes the necessity to accurately model the initial section.

Wen and Yoshida have suggested that the only criterion required in determining the effects of the first section height on the overall model performance is the kinetic speed of the reaction, i.e., the value of the rate constant k_c . They conclude from their results that the overall conversion for a fast reaction is not effected by the value of ΔH_1 and, therefore, no effect will be seen for reactions having low rate constants.

In Figures 17 and 18 gas concentration profiles for Runs 1 and 12 are plotted. These two runs represent the extremes in experimental conversions which were investigated. Run 1 is kinetically the faster of the two; having a $k_c = 6.56 \times 10^{-2}$ ft/sec compared with $k_c = 0.328 \times 10^{-2}$ ft/sec

TABLE VII
SOLID CONCENTRATION DATA

Run No.	Initial Conc. mole/ft. ³	Avg. Conc. Leaving 1 st Section	Avg. Conc. Leaving Top Section
1	2.22	4.3×10^{-4}	2.5×10^{-4}
2	2.22	1.0×10^{-3}	7.6×10^{-4}
6	3.58	8.7×10^{-2}	8.6×10^{-2}
10	3.58	1.0×10^{-1}	9.9×10^{-2}

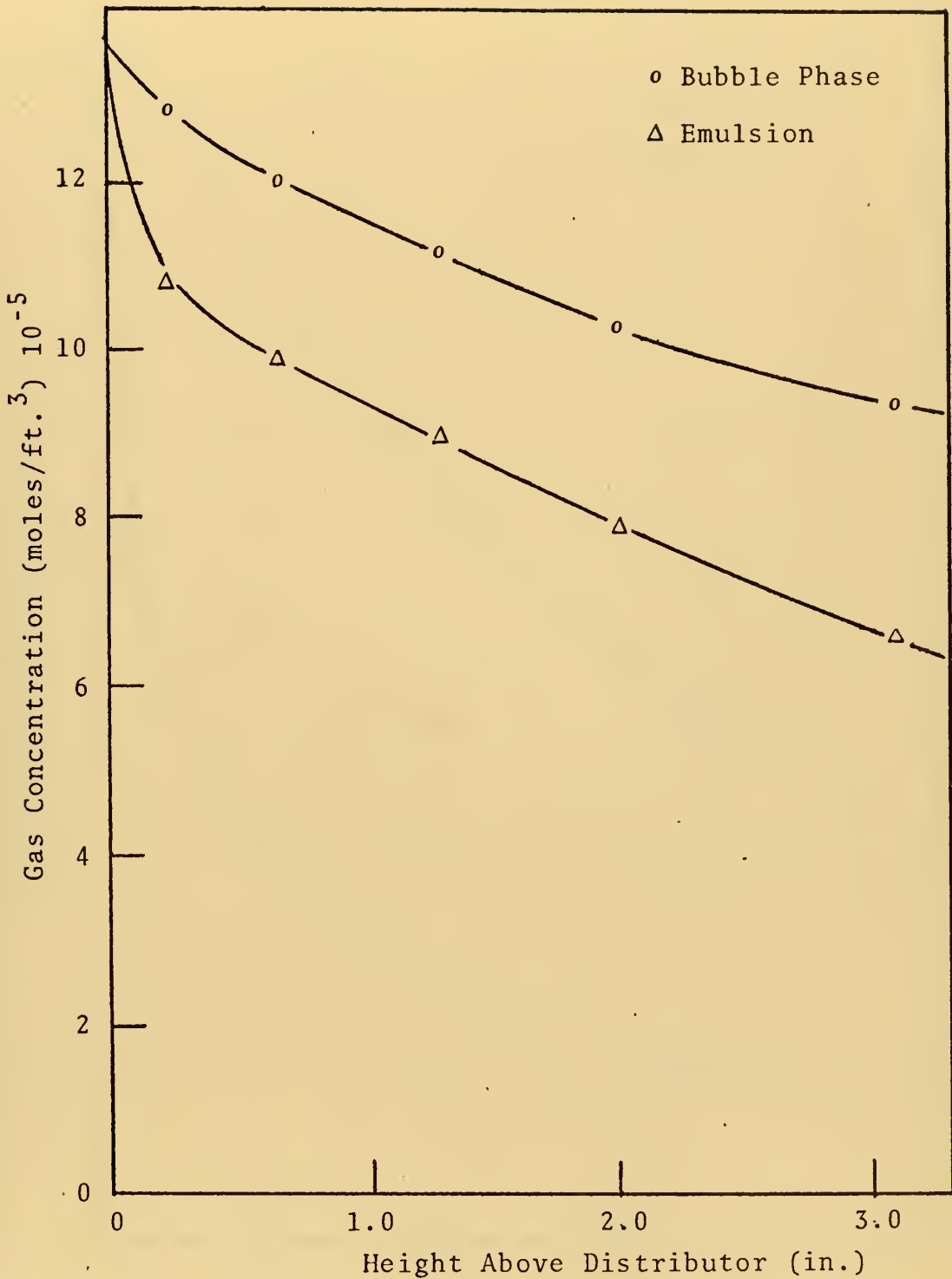


Figure 17. Gas Concentration Profiles for Run 1;
 ΔH_1 Based Cloud Size.

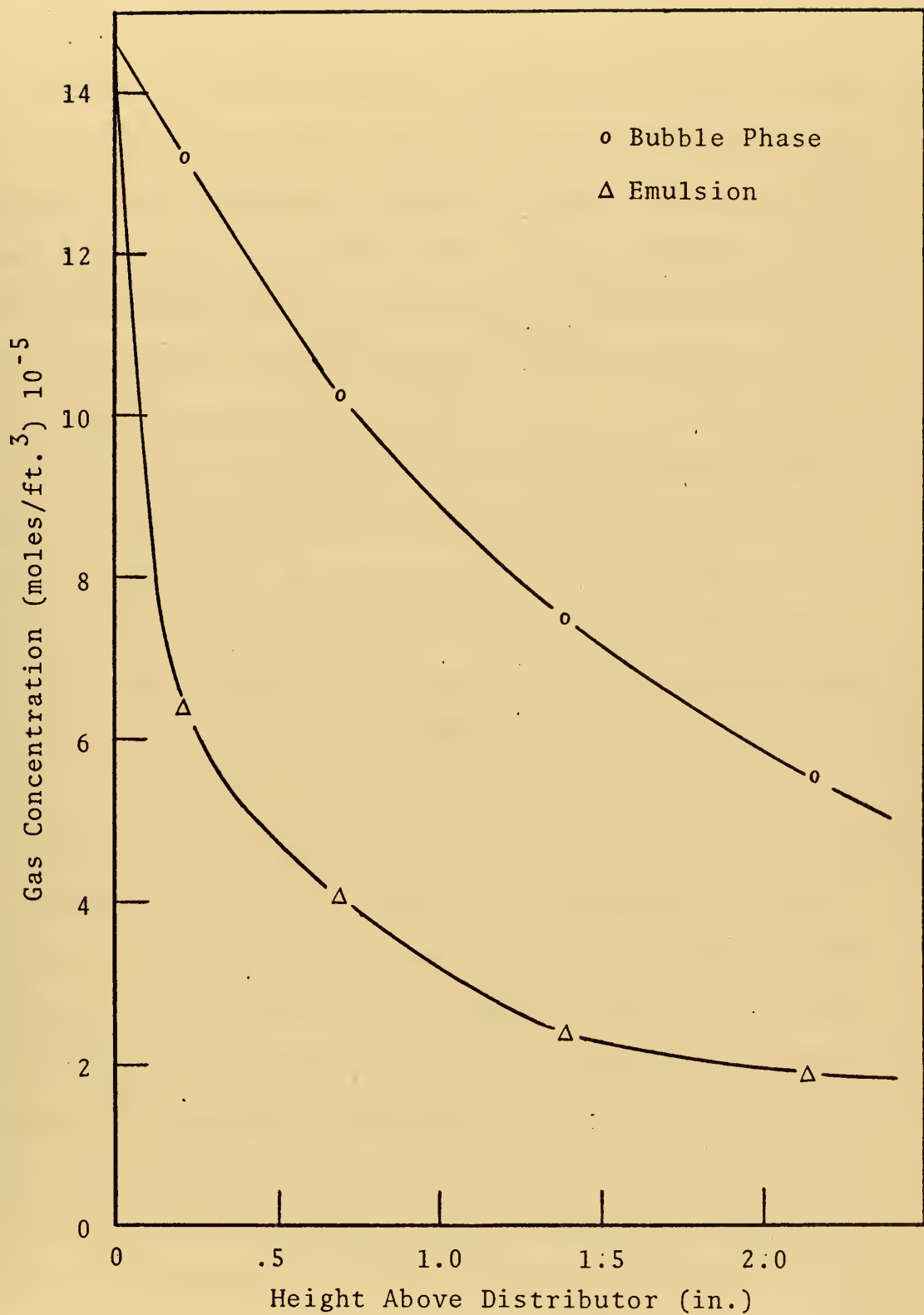


Figure 18. Gas Concentration Profiles for Run 12;
 ΔH_1 Based on Cloud Size.

for Run 12. The figures show that gas concentrations for the kinetically slower reaction change more rapidly in the initial height of the bed than do the concentrations for the more rapid reaction. The emulsion gas concentration showed a very rapid drop for Run 12. At a height of 0.5 in. from the distributor, a 71% decrease in emulsion gas concentration was found. This compares to a 27% change in the emulsion gas concentration for Run 1.

The effect on the overall conversion resulting from a change in the initial section height for Runs 1 and 12 is shown in Figure 19. As suggested by the gas concentration profiles, Run 12 shows a sensitivity to ΔH_1 , while Run 1 does not. This trend is not expected if Wen's and Yoshida's conclusion that slow reactions are not sensitive to the value of ΔH_1 is accepted.

In Run 12, the reactant feed rate and the initial reactant concentration of the feed were substantially larger than Run 1. The fact that the conversions in Run 12 were sensitive to the value of ΔH_1 suggests that the feed rate and initial concentration as well as the value of the rate constant are important parameters in determining the effect of ΔH_1 on the overall bed conversion.

Runs 10, 11, and 12 were used to study this effect. These runs represent a series in which all parameters except the feed rate are constant. The feed rate increases for this series of runs.

In Figure 20, normalized average gas concentrations are plotted for the three runs. As the feed rate of the solid

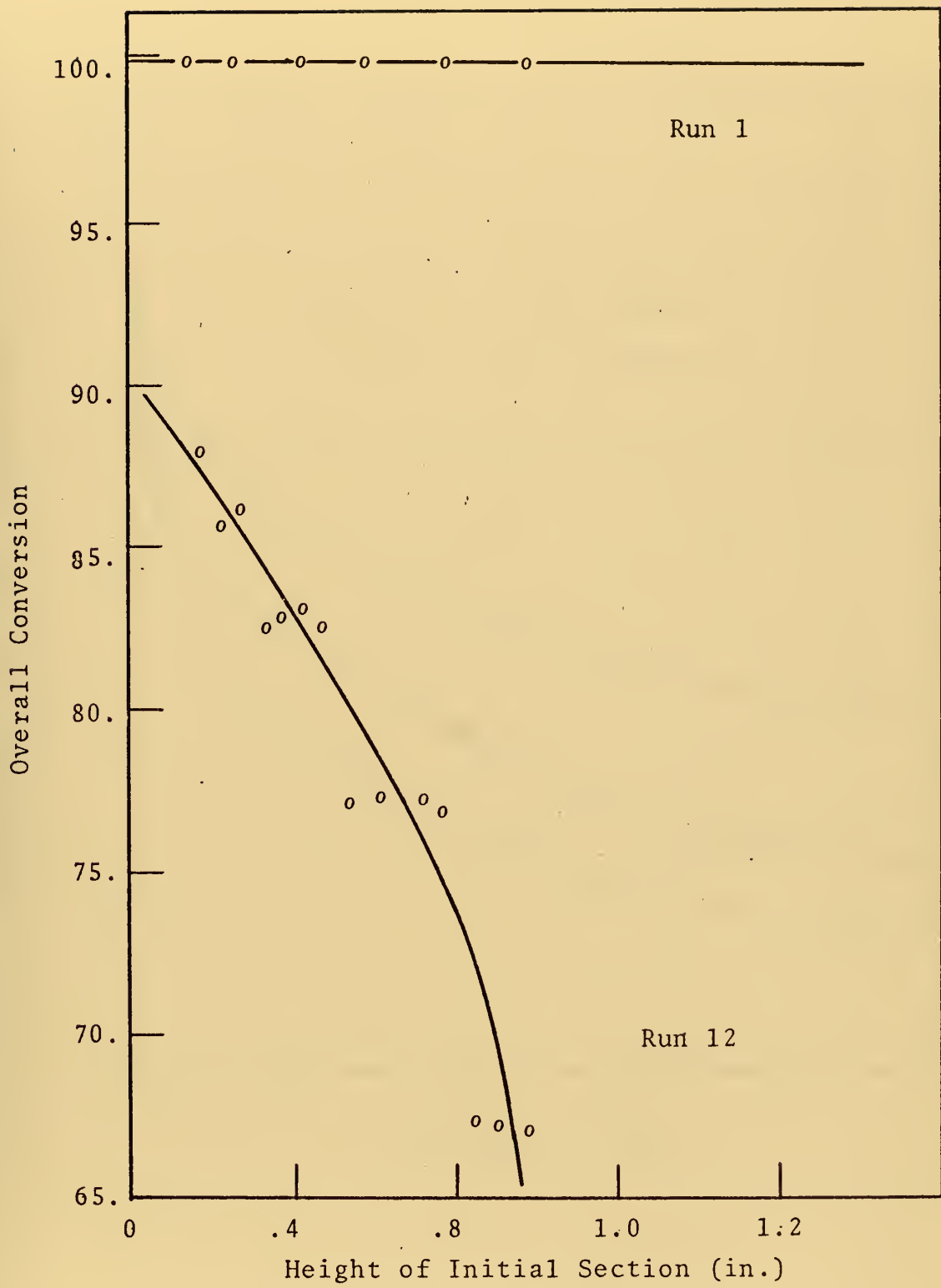


Figure 19. Conversion Versus ΔH_1 Runs, 1, 12.

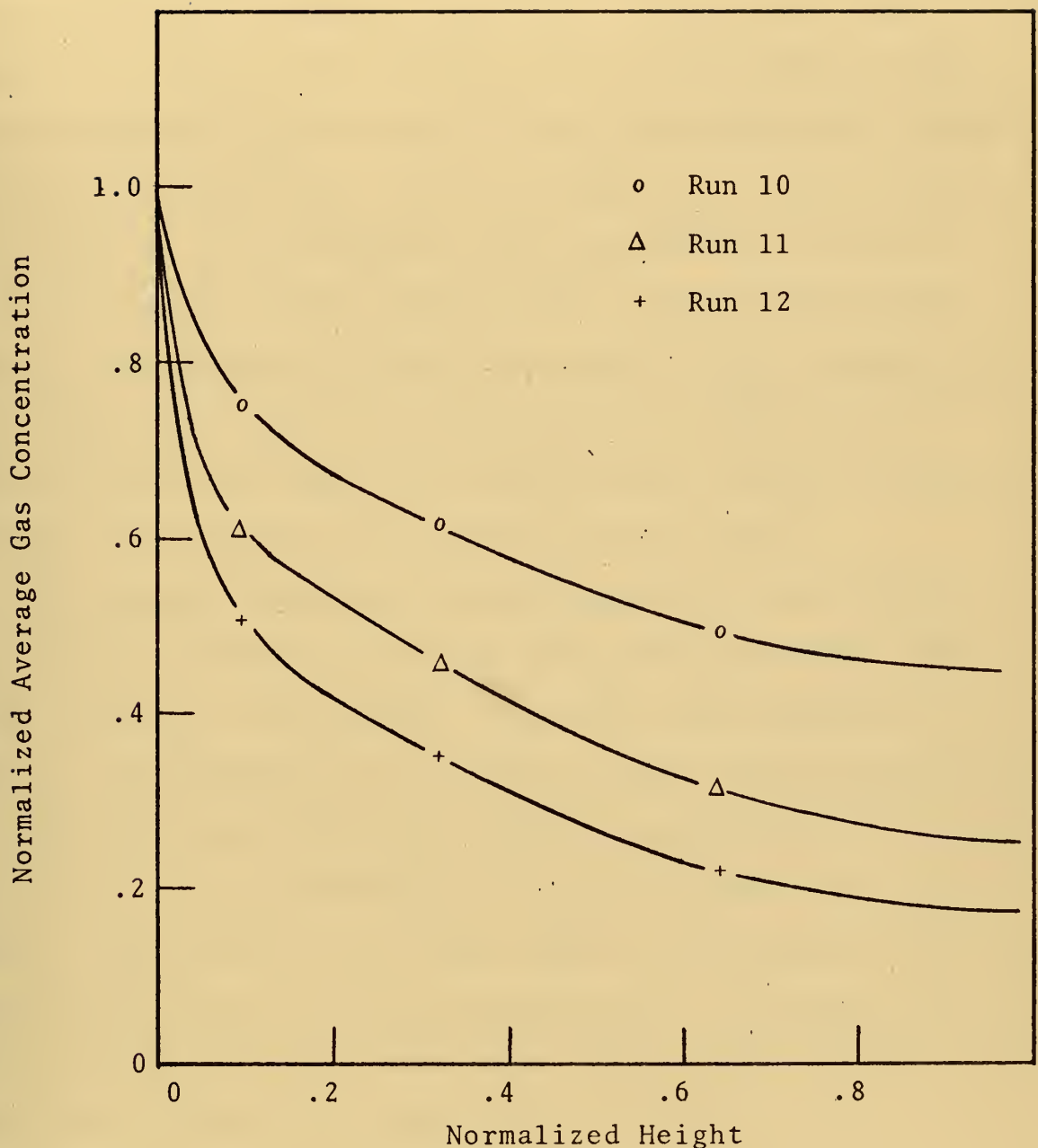


Figure 20. Normalized Gas Concentration Profiles Runs 10, 11, 12.

to the bed increases, conversion and average gas concentrations decrease as would be expected. All the runs show rapid gas concentration changes near the distributor plate which suggests that the value of ΔH_1 will effect the overall calculated conversion. This was found to be true as shown in Figure 21. Run 12 showed the greatest sensitivity to a change in the initial section size. The conversion for Run 12 decreased by 21% over the range of ΔH_1 . For Run 11, the change was only 15% and for Run 10, it was only 5%. These results show that the feed rate does effect the sensitivity of the model to the initial value of ΔH_1 .

The complete meaning of this conclusion is not clear, but some speculation concerning the reasons for this feed rate dependency can be made. The fact that conversion was found to be dependent on the value of ΔH_1 can be interpreted to mean that the model will predict experimental conversions accurately if correct values of ΔH_1 are known. This logic ignores the fact that the model might still predict incorrect conversions due to its not accounting for a residence time distribution of solids within the bed, an effect which was previously shown to be significant.

From Figure 21, the values of ΔH_1 , for which the model will predict the correct experimental conversions can be read. The values are: Run 10, > 1.0; Run 11, 0.88; and Run 12, 0.83 in. The interesting fact is that ΔH_1 is different for the three runs and decreases as the feed flow rate is increased. One would expect that for the same gas

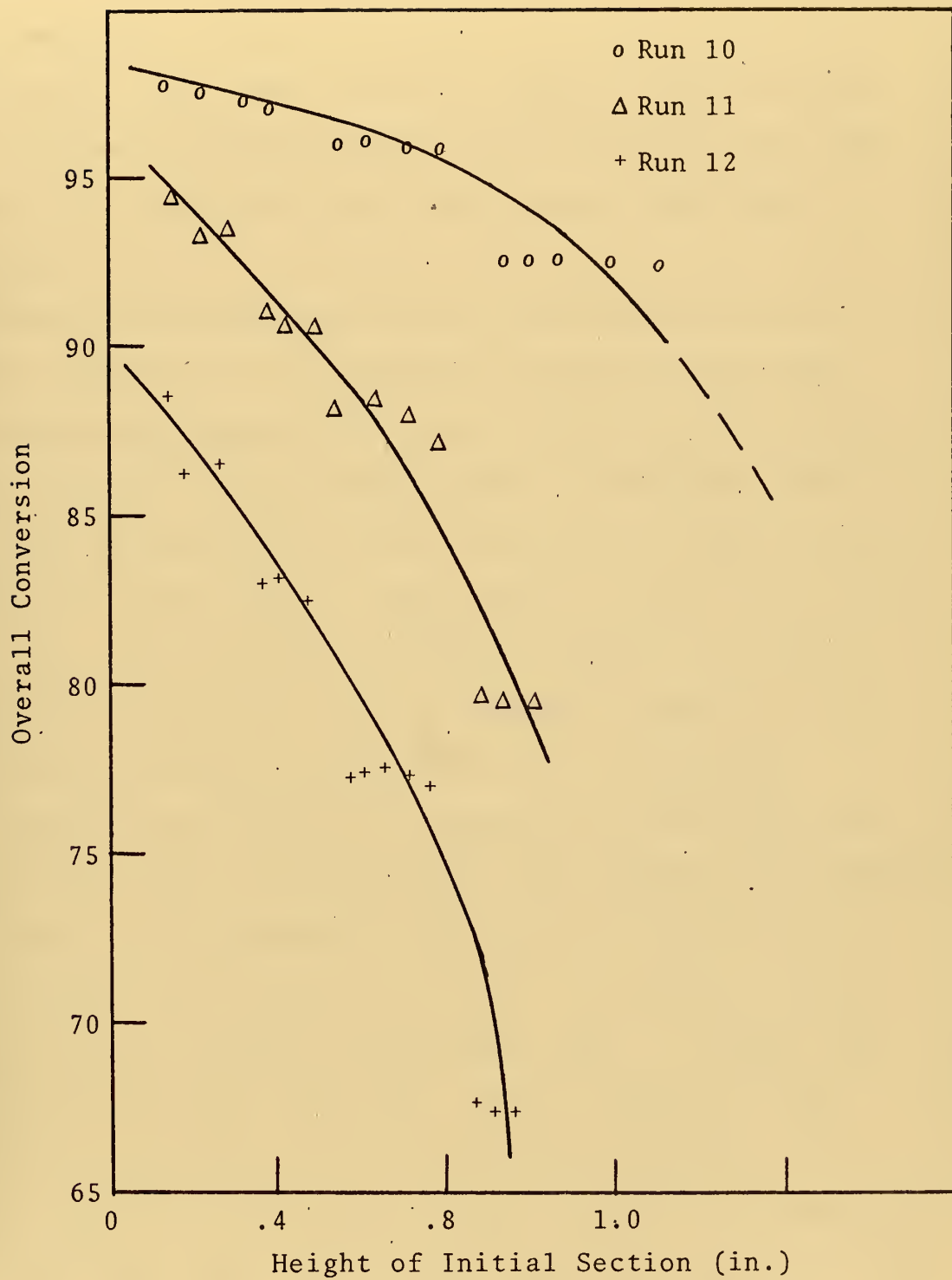


Figure 21. Conversion Versus ΔH_1 Runs 10, 11, 12.

flow conditions, bubbles of equal size would form at the distributor. The trend, however, suggests that different size bubbles are being formed at the distributor and that their size is dependent upon the reaction conditions in the bed.

Recent investigation [37] into the mechanics of the bubble formation at distributors in fluidized beds have shown that very small bubbles are initially formed, which because of their large inertia swirl in turbulent jets just above the distributor surface. These small bubbles rapidly coalesce and form large, stable bubbles at the tips of the gas jets. If this model of bubble formation is correct, a dependence between the size of the bubbles formed at the jets and the reaction conditions is not surprising.

Consider the effects of increasing the feed flow rate to the bed. This action increases the tendency for reaction and thus the disappearance of gas from the bubble phase. As a result, two effects will occur: 1) smaller, stable bubbles will be formed by coalescence and, 2) sharper gas concentration drops will occur. These trends are both present in the data plotted in Figures 20 and 21; a fact which supports the speculative logic used in the analysis. The conclusion that can be drawn from these results is that the uncertainty in the existing mechanism of bubble formation could possibly be the controlling factor in the development of a successful mathematical model of fluidized bed operations.

V. CONCLUSIONS AND RECOMMENDATIONS

The major conclusions of this investigation are:

1. The conversions predicted by the proposed model are significantly higher than the experimental values of Yagi et al [34]. The average percent error of the predicted conversions was 8.3%.
2. The results are not dependent on the method used for calculating the section heights. Conversions obtained from the model when the section heights were based on the cloud diameter were essentially identical to the conversions predicted by the model when the section heights were based on the bubble diameter alone.
3. The assumption that the bed solids have a uniform residence time equal to \bar{t} , which ignores a solid residence time distribution, contributes to the calculation of conversions which are higher than experimental values. Calculations using the residence time distribution concept and the average gas concentration predicted by the model show a significant improvement in the overall results. For these calculations, the average percentage error was reduced to 5.08%. Modification of the model material balances to include the residence time distribution concept is recommended.
4. Investigation into the effects of having to assume the height of the initial reactor section indicate that the

overall conversion results are dependent upon the assumed value (ΔH_1). Large changes in the solid and gas concentrations in the initial section support this conclusion. The sensitivity of the predicted conversions to the value of ΔH_1 was found to be a function of the kinetic rate constant and the feed rate of solid reactant. The trends indicate that the sensitivity increases for decreasing rate constants and for increasing feed flow rates.

The model proposed in this investigation represents the first step in the development of a mathematical model for use in the design and study of fluidized bed reactors for the combustion of solid wastes. Modification to include the concept of a solid residence time distribution is required. Furthermore, complete understanding of the mechanism of bubble formation at the surface of the distributor in a fluidized bed is essential in light of the observed dependence between the overall conversion and the initial section height. For use in the study of combustion type reactions, modification for handling the kinetics of shrinking particles must also be made. In this regard, the concepts proposed by Kunii and coworkers [15,38] are recommended.

APPENDIX A
TERMINAL VELOCITY CALCULATION

The terminal velocity of the bed particles was calculated using the equations derived by Leva [39].

$$U_T = \frac{(\rho_p - \rho_g) g D_p^2}{18 \mu'} \quad Re < 2.0 \quad (56)$$

$$U_T = \frac{0.152 D_p^{1.14} g^{.714} (\rho_p - \rho_g)^{.714}}{\mu^{.428} \rho_g^{.285}} \quad 20 < Re < 500 \quad (57)$$

$$U_T = \left[\frac{3g D_p (\rho_p - \rho_g)}{\rho_g} \right]^{.5} \quad Re > 500 \quad (58)$$

APPENDIX B

CHARACTERISTICS AT MINIMUM FLUIDIZATION

The bed voidage at minimum fluidization was calculated from the data of Agarwal and Storrow [41]. The ϵ_{MF} was found by these investigators to be a function of the particle diameter and the bed material. Their data for soft brick particles is shown in Figure 22. This data was fitted to three straight lines. The correlation coefficients of $\pm 99\%$. The equations are

$$D_p \leq 0.003$$

$$\epsilon_{MF} = -38.0D_p + 0.613 \quad (59)$$

$$0.003 < D_p \leq 0.006$$

$$\epsilon_{MF} = 015.8 D_p + 0.542 \quad (60)$$

$$D_p \geq 0.006$$

$$MF = -4.18 D_p + 0.474 \quad (61)$$

The minimum fluidization velocity was calculated from an equation given by Kunii and Levenspiel [15]. For small particles this equation is

$$UMF = \frac{D_p^2 (\rho_p - \rho_s) g}{1650 \mu'} \quad (62)$$

The gas viscosity and density required for this calculation were calculated at the bed temperature and atmospheric pressure from the equations

$$\rho g = \frac{PM}{RT'} \quad \text{IDEAL GAS LAW} \quad (63)$$

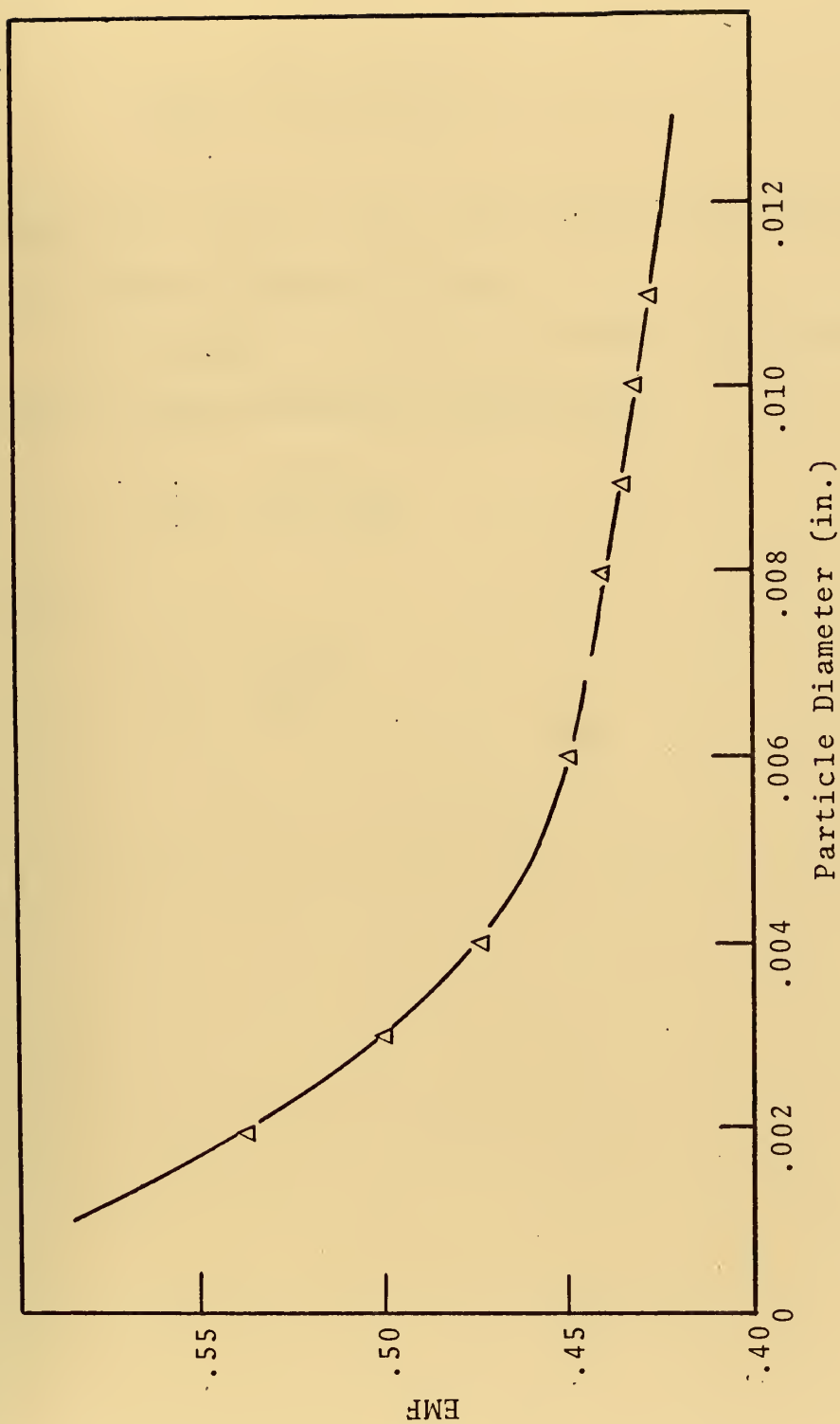


Figure 22. EMF Data.

$$\mu_{i1} = \mu_{i2} \left(\frac{T'_2}{T'_1} \right)^{3/2} \frac{T'_1 + 1.47 T_B}{T'_2 + 1.47 T_B} \quad (64)$$

$$\mu_{mix} = \frac{\sum y_i \mu_i (M_i)^{1/2}}{\sum y_i (M_i)^{1/2}} \quad (65)$$

Equations (64) and (65) were obtained from Perry's Handbook for Chemical Engineers [41].

The height of the bed at minimum fluidization was calculated from the EMF by the equation

$$HMF = \frac{12 H_o}{1.0 - \epsilon_{MF}} \quad (66)$$

where

$$H_o = \frac{144 W_t}{\rho_p S_t} \quad (67)$$

APPENDIX C

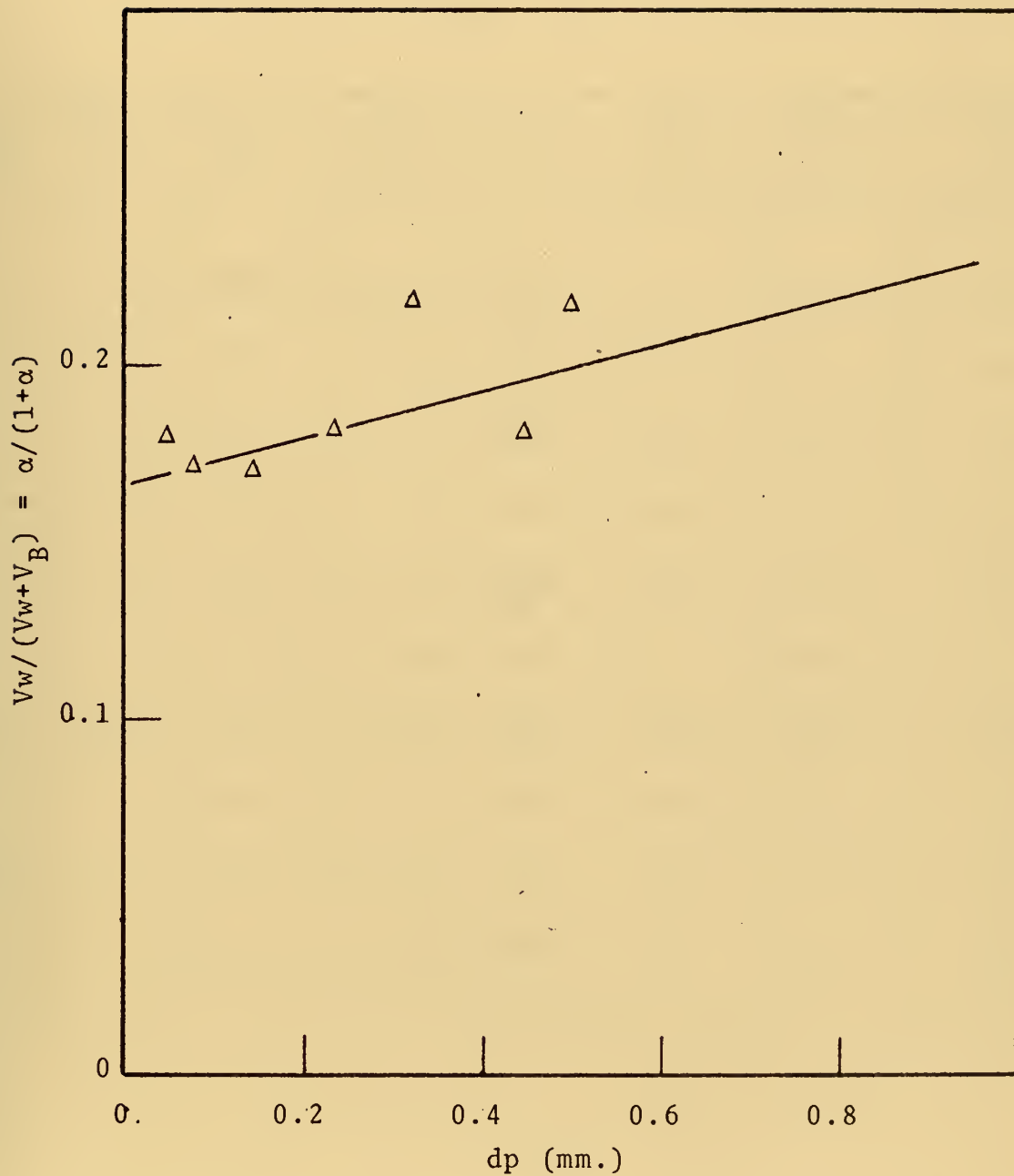


Figure 23. Plot of Data for Determination of the Wake Volume.

APPENDIX D

TABLE VIII

INPUT DATA

Run No.	D _p x 10 ⁻³ in.	Temp. °F	W _f x 10 ⁻⁵ lb/sec	U ft/sec	k _c x 10 ⁻² ft/sec	C _{G₀} x 10 ⁻⁴ mole/ft ³	C _{S₀} mole/ft ³
1	4.33	1652.	6.65	.6562	6.56	1.361	2.22
2	4.33	1652.	9.941	.6562	6.56	1.361	2.22
3	3.50	1292.	3.674	.6365	.328	1.648	3.577
4	3.50	1382.	7.458	.6365	.984	1.561	3.577
6	3.50	1382.	11.023	.6365	.984	1.561	3.577
7	3.50	1472.	7.349	.6365	1.97	1.486	3.577
10	3.50	1292.	7.349	.6365	.3281	1.648	3.577
11	3.50	1292.	11.023	.6365	.3281	1.648	3.577
12	3.50	1292.	14.680	.6365	.3281	1.648	3.577
13	3.50	1382.	3.895	.6693	.984	1.561	3.577

APPENDIX E
MODIFIED SECTION HEIGHT CALCULATION

The cloud diameter surrounding a bubble of size DB can be calculated from the relation proposed by Davidson [29]

$$DC = DB \left[\frac{U_{BR} + 2 UMF/\epsilon_{MF}}{U_{BR} - UMF/\epsilon_{MF}} \right]^{1/3} \quad (68)$$

In order to define a section height (ΔH) on the basis of the cloud diameter, an averaging procedure similar to that employed previously was used. Using this procedure, the average section bubble diameter was defined as

$$DB_N = \frac{XM \sum^N H + Do}{1 - XM/2} \quad (69)$$

On this basis, the section height based on the cloud diameter can be written as

$$\Delta H_N = DB_N \left[\frac{U_{BR} + 2 UMF/\epsilon_{MF}}{U_{BR} - UMF/\epsilon_{MF}} \right]^{1/3} \quad (70)$$

When this formulation is used, the number of bubbles in each section becomes

$$N = \frac{6 S_T (H - HMF) \Delta H_N}{\pi H DB_N} \quad (71)$$

COMPUTER PROGRAM

MAJOR COMPUTER VARIABLES

NOTE VARIABLE NAMES NOT LISTED BELOW ARE MINOR VARIABLES WHICH RESULT WHEN THE MAJOR VARIABLES ARE COMBINED FOR SIMPLIFICATION PURPOSES.

UNITS ARE AS GIVEN IN THE TABLE OF SYMBOLS UNLESS OTHERWISE STATED.

ALPHA	WAKE VOLUME/BUBBLE VOLUME
AREAB	REACTOR PHASES AREA
AREA1	REACTOR CROSS SECTIONAL AREA
B	STOICHIOMETRIC COEFFICIENT
CCB	BUBBLER PHASE CONCENTRATION
CCBAR	AVERAGE GAS CONCENTRATION
CCBED	AVERAGE BED GAS CONCENTRATION
CGE	EMULSION GAS CONCENTRATION
CGO	INITIAL GAS CONCENTRATION
CGUESS	INITIAL GUESS OF CGB(N)
CNORM	NORMALIZED GAS CONCENTRATION
CONBED	OVERALL CONVERSION FROM BACKMIXED EQUATIONS
CONS	KINETIC RATE CONSTANT BASED ON SOLID VOLUME
CONVEX	EXPERIMENTAL CONVERSION
CONVT	TOTAL BED CONVERSION
CS	SOLID CONCENTRATION
CSO	INITIAL SOLID CONCENTRATION
CSRST	CLOUD SOLIDS DISTRIBUTION FUNCTION
CTEST	CLOUD SOLID CONCENTRATION FUNCTION
D1,D2,D3	CALCULATED DIFFERENCES USED IN RCORE SEARCH
DBAVG	AVERAGE BUBBLE DIAMETER
DBMAX	MAXIMUM BUBBLE DIAMETER
DCMAX	MAXIMUM CLOUD DIAMETER
DELB	BUBBLE DIAMETER
DELG	INCREMENT IN THE GAS SEARCH

DELTAH SECTION HEIGHT OF THE INERTS
 DENS1 DENSITY OF THE INERTS
 DENSG GAS DENSITY
 DIA1 REACTOR DIAMETER IN
 DIA1 DIAMETER OF THE BED SOLIDS (INERTS)
 DIFH RESIDUAL HEIGHT IN THE TOP SECTION
 DOCGS INITIAL BUBBLE SIZE CM.
 DP DIAMETER OF BED SOLIDS
 DZERO INITIAL BUBBLE SIZE IN
 DEMF MINIMUM FLUIDIZATION VOIDAGE
 ERROR ABSOLUTE VALUE IN THE PREDICTED ERROR
 EESR EMULSION SOLIDS DISTRIBUTION FUNCTION
 GEX GAS EXCHANGE EQUALS EXCHANGE COEFFICIENT
 GMAX, GMIN THE BUBBLE VOLUME
 MAXIMUM AND MINIMUM GAS CONCENTRATION
 FOR SEARCH LOOP .

HF BED HEIGHT
 HGRAPH TOTAL BED HEIGHT (HTOTAL)
 HINT HEIGHT OF BED USED FOR GRAPHING
 HMFE INITIAL SECTION HEIGHT
 HMFN HEIGHT OF BED AT MINIMUM FLUIDIZATION
 HNORM NORMALIZED HEIGHT
 HZERO MINIMUM BED HEIGHT ($E=0$)
 PCERR PERCENT ERROR IN OVERALL CONVERSION
 PERCENT ERROR IN THE CALCULATED INITIAL
 GAS CONCENTRATION

RADB BUBBLE RADIUS
 RADC CLOUD RADIUS
 RATEK CONSTANT
 RMAX,RMIN MAXIMUM AND MINIMUM CORE SIZE
 RZERO INITIAL REACTANT RADIUS
 TAUBED OVERALL TIME FOR COMPLETE REACTION

TEMP TEMPERATURE DEGREES KELVIN
 TREBED OVERALL PARTICLE RESIDENCE TIME
 TRES SECTION PARTICLE RESIDENCE TIME
 TSUPERFICIAL GAS VELOCITY AT THE BED TEMP.
 UBMX MAXIMUM BUBBLE VELOCITY
 UBRE AB SOLUTE BUBBLE RISE VELOCITY
 UBREL RELATIVE RISE VELOCITY
 UMF0 MINIMUM FLUIDIZATION VELOCITY
 UMFO MINIMUM FLUIDIZATION VELOCITY AT 20 DEGREE
 UOFO SUPERFICIAL GAS VELOCITY AT 20 DEGREES
 UTERM PARTICLE TERMINAL VELOCITY
 UVOL VOLUMETRIC GAS FLOW RATE

VBB BUBBLE VOLUME IN THE TOP SECTION
 VBFR FRACTIONAL BUBBLE VOLUME IN THE TOP SECTION
 VBI VOLUME OF A SINGLE BUBBLE


```

***** CLOUD VOLUME IN THE TOP SECTION
VCFR FRACTIONAL CLOUD VOLUME IN THE TOP SECTION
VCORE CORE VOLUME
VC1 VOLUME OF A CLOUD IN THE TOP SECTION

VE EMULSION VOLUME
VISCG GAS VISCOSITY CENTIPOISE
VISCN2 GAS VISCOSITY LBS./FT. SEC
VISO2 VISCOSITY OF NITROGEN CENTIPOISE
VISO2 VISCOSITY OF OXYGEN CENTIPOISE
VOID BED VOIDAGE
VTR FRACTIONAL VOLUME IN THE LAST SECTION
VT1 FRACTIONAL VOLUME OF A SINGLE BUBBLE CLOUD
ENTITY IN THE TOP SECTION
VZERO INITIAL PARTICLE VOLUME
WB BUBBLE PHASE SOLID FLOW
WE EMULSION PHASE SOLID FLOW
WFEED SOLID FEED RATE LBS./SEC
WTMOL MOLECULAR WEIGHT OF THE SOLID
WTMOL MOLECULAR WEIGHT OF THE GAS
XF CROSS FLOW COEFFICIENT
XLBS WEIGHT OF SOLIDS IN THE BED
XN CONSTANT
XNB NUMBER OF BUBLES PER UNIT AREA IN THE DISTRIBUTOR
XNO NUMBER OF HOLES PER UNIT AREA IN THE DISTRIBUTOR
*****
```

```

IMPLICIT REAL*8(A-H,O-Z)
DIMENSION DEL(20),CGBAR(20),HNORM(20),CNORM(20),PROD(20)
*CSR(20),CGE(20),CS(20),TAU(20),GEX(20),ESR(20),
*TRES(20),WE(20),WB(20)
C*****READ INPUT VARIABLES
C*****READ(5,1) DIA,XNO
FORMAT(5,1) DIA,F10.3
1  READ(5,2) XLBS,DIA1,DENS1,RZERO
FORMAT(5,2) F10.2,F10.3
2  READ(5,3) TEMP,B,RATEK,WTMOL
FORMAT(5,3) F10.5
3  READ(5,4) WFEED,CSO,U0,CGO
FORMAT(5,4) F20.8
4  READ(5,5) ALPHA,HINT,CONVEX
FORMAT(5,5)
```



```

20      WRITE(6,20) T60, 'INPUT PARAMETERS')
FORMAT(6,30) T52, 'EQUIPMENT PHYSICAL CHARACTERISTICS')
30      WRITE(6,40) DIA, XNO
FORMAT(6,40) T58, 'REACTOR DIAMETER= ', F6.2, T83, 'IN.', /, T58, 'DISTRIBUTION'
40      * TOR HOLES PER SQ. FT.=, F6.3)
FORMAT(6,50) T52, 'BED CHARACTERISTICS')
WRITE(6,60) XLBS, 'WT. OF INERTS', F7.2, T82, 'LBS.', /, T58, 'DIA. OF INDAL
FORMAT(6,60) T58, 'WT. OF INERTS', F7.2, T82, 'LBS.', /, T58, 'DENSITY OF INERTS'
60      * F7.6, T82, 'IN.', /, T58, 'DENSITY OF REACTANT= ', F7.3, T87, 'LBS./CUBIC FT.'
* CUBIC FT./T58, 'DENSITY OF REACTANT= ', F8.5, T87, 'IN.')
FORMAT(6,70) T52, 'OPERATIONAL PARAMETERS')
70      WRITE(6,80) TEMP, 'TEMPERATURE= ', F6.1, T78, 'F', /, T58, 'SUPERFICIAL VEL
FORMAT(6,80) F8.6, T88, 'FT./SEC.')
80      * F8.1) WFEED, 'SOLIDS FEED RATE= ', G10.5, T86, 'LB./SEC.')
FORMAT(6,81) T58, 'SOLID CONCENTRATION= ', F10.5, T89, 'LB MOLES/CUBIC FT.')
81      WRITE(6,82) CGO, CSO
FORMAT(6,82) T58, 'GAS CONCENTRATION= ', F10.5, T89, 'LB MOLES/CUBIC FT.')
82      * FT., /, T53, 'SOLID CONCENTRATION= ', F10.5, T89, 'LB MOLES/CUBIC FT.')
C***** TERMINAL VELOCITY AND MAXIMUM BUBBLE SIZE CALCULATION ****
C***** TEST=DP*(3.2*2*DENSG*(DENSI-DENSG)/VISCV)*0.333
C***** TEST=LE*2.3) GO TO 84
C***** IF(TEST>4.3*6) GO TO 83
C***** UTERM=0.153*32.2**0.71*DP**1.14*(DENSI-DENSG)**0.71/(DENSG**0.29
C***** * VISCV*0.43)
C***** GO TO 85
C***** AUG=3.2*2*DP*(DENSI-DENSG)/DENSG
C***** UTERM=1.74*DSQRT(AUG)
C***** GO TO 85
C***** UTERM=32*2*DP**2*(DENSI-DENSG)/(18.0*VISCV)
84      IF(U*GE.*UTERM) GO TO 948
85      DBMAX=0.373*(UTERM/0.711)**2
      UBMAX=0.711*DSQRT((32*2*DBMAX/12.0)
FACTOR=(UBMAX+2.0*UMF/EMF)/(UBMAX-UMF/EMF))**2
* (1.0/3.0)
DCMAX=DBMAX*FACTOR

```



```

C***** MISCELLANEOUS CALCULATIONS ****
C***** ****
C
      DIAR=2.0*RZERO/12.0
      XM=0.684*DENS1*DP*(U0/UMFO)
      IF(XM.GE.2.0) GO TO 940
      IF(XNO.EQ.0.000) GO TO 90
      XNOCGS=XNO/929.03
      DOCCS=(158.3*(U-UMF)/XNOCGS)**0.4)/(980.0)**0.0
      DZERO=DOCCS/2.54
      GO TO 200
CONTINUE
      DZERO=(2.0-XM)*HINT/2.0
      DBAVG=6.0*XN*HMF+DZERO
      IF(DBAVG.LE.DBMAX) GO TO 210
      DBAVG=DBMAX
      HF=HMF*((U-UMF)/(0.711*(32.2*DBAVG/12.0)**0.5))+HMF
      HTOTAL=12.0*HF
C***** DATA OUTPUT FORMAT ****
C***** ****
C
      WRITE(6,222) 'INTERNAL PARAMETERS'
      222  FORMAT(1I24) VISC,DENSG,EMF
      223  FORMAT(1I24) T56,VISCG,DENS,G15.6,T80,'CP',/,T56,'DENSG= ',G15.6,T80,
      224  *     'LBS./CUBIC FT',/T56,'EMF=G15.6}
      *     WRITE(6,226) UMF,HZERO,UMF
      226  FORMAT(1I24) T56,UUMF=,G15.6,T80,'FT./SEC',/,T56,'HZERO= ',G15.6,T80,'FT.='
      *     80,FF=,T56,HMF=,G15.6,T80,'FT.='
      227  FORMAT(1I24) T56,FF=G15.6,T80,'FT.'
      228  FORMAT(6,228) UTERM,DENAX,DZERO
      229  FORMAT(1I24) T56,UTERM=,G15.6,T80,'FT./SEC',/,T56,'DBMAX= ',G15.6
      *     T80,IN=,T56,DZERO=,G15.6,T80,IN)
      230  FORMAT(1I24) T56,HINT=G15.6,T80,IN)
      231  FORMAT(6,230) XM,DBAVG,RATEK
      232  FORMAT(1I24) T56,XM=G15.6,T80,'FT./SEC')
      *     RATEK=G15.6,T80,'FT./SEC')
      233  FORMAT(6,232) T32,SECT.,T14,HEIGHT,HT.,T32,SECT.,T14,HEIGHT,HT-GRAPH')
      234  FORMAT(6,234) T4,NO.,T18,IN.,T33,IN.,T51,IN.)

```



```

C***** SECTION CALCULATIONS *****
C***** *****
C      H=0.0
C      K=0
C      INDEX=1
C      SUM=0.0
C      IFLAG=1
238   DO 900 N=1,50
        IF (N>38) LOOP=1
        SUM=SUM+DEL(IFLAG)
        CONTINUE
        DELB=(XM*SUM+DZERO)/(1.0-XM/2.0)
        UBREL=0.711*DSQRT(32.0*DELB/12.0)
        FACTOR={(UBREL+2.0*UMF/EMF)/(UBREL-UMF/EMF)})**
        *{(1.0/3.0)*DELTAH=DEL B*FACTOR
        DEL(N)=DELTAH
        IFLAG=IFLAG+1
        SUM=0.0
        GO TO 241
        DELB=HINT
        UBREL=0.711*DSQRT(32.0*2*DEL B/12.0)
        FACTOR={(UBREL+2.0*UMF/EMF)/(UBREL-UMF/EMF)})**
        *{(1.0/3.0)*DELTAH=DEL B*FACTOR
        DEL(N)=DELTAH
        IF(DELTAH.LT.DCMAX) GO TO 250
        DELTAH=DCMAX
        K=K+1
        DELH=DELTAH
        HGRAPH=H+DELTAH/2.0
        HNORM(N+1)=HGRAPH/HTOTAL
        ZH=2.54*H
        FUNX=62.40*DELTAH*UMF/(DENSI*DIAI*U)
        XH=HGRAPH/12.0
        R=HMF*(1.0-R)/HF
        VOID=1.0-R
240   XNBI=144.0*AREA
        XNB(I)=(6.0*AREA*I*DELTAH/(3.14*DEL B**3))*
        **(VOID-EMF)/(1.0-EMF)
        IF(K.LE.1) GO TO 520
        XNB(I)=XNB(I-1)

```



```

520 IF(UBREL.LE.UMF/EMF) GO TO 945
      UBR=U-UMF+UBREL
      VB=3.14**XNB((I)*DELB**3/6.0
      VC=VB*(3.0*UMF/(EMF*UBREL-UMF))
      VE=AREAI*DELTAH-VB-VC
      XF=4.331/DELB
      AREAB=0.785*XNB((I)*DELB**2/144.0
      GEX(N)=VE*(1.0-EMF)/1728.0
      CSR(N)=(VC+ALPHA*VB)*(1.0-EMF)/1728.0
      WBN=(WFEED/(DENSR*AREA))*AREAB+ALPHA*AREAB*UBR
      WE(N+1)=ALPHA*AREAAB*UBR-(WFEED/(DENSR*AREA))*(AREA-AREAB)
      TRES(N)=(ALPHA*VB+VC+VE)*(1.0-EMF)/(WFEED*1728.0/DENS)
      *+WE(N+1)) GO TO 570
      * IF(H*LE*12*0*HF) GO TO 570
      HNORM(N+1)=1.0
      HTOTAL=DELTAH
      H1=HTOTAL
      HGRAPH=HTOTAL
      DIFH=12.0*HF-H1
      DELH=DIFH
      VBI=VB/XNB(I)
      RADB=DELB/2.0
      VC1=VC/XNB(I)
      VT1=VC1+VBI
      RADC=DELTAH/2.0
      IF(DIFH/DELTAH.LE.0.5) GO TO 562
      VBF=VB1-1.0472*(DELTAH-DIFH-RADC+RADB)**2*
      *(12.0*RADB-DELTAH+DIFH+RADC)
      *(3.0*RADC-DELTAH+DIFH)**2*
      VCFR=VTFR-VBFR
      VC=VCFR*XNB(I)
      GO TO 563
      VBF=1.0472*(DIFH-RADC+RADB)**2*(3.0*RADC-DIFH)
      VCFR=VTFR-VBFR
      VE=AREAI*DIFH-VC
      R=HMFF*(1.0-EMF)/HF
      VOID=1.0-R
      GEX(N)=XF*VB/1728.0
      CSR(N)=VE*(1.0-EMF)/1728.0
      CSR(N)=(VC+ALPHA*VB)*(1.0-EMF)/1728.0
      WB(N)=0.0
      WE(N+1)=0.0
      TRES(N)=(ALPHA*VB+VC+VE)*(1.0-EMF)/(WFEED*1728.0/DENS)

```



```

*+WE(N+1))
 570  WRITE(6,800) N,DELT,H,HGRAPH
 800  FORMAT(0,14,F20.4,2F16.4)
  IF(KGT-1) GO TO 835
  WRITE(6,810) VOID,UBREL,UBR
  FORMAT(0,T58,VOID,UBREL,UBR
  *      ,T58,6,T58,FT/SEC,;G15.6,T58,UBREL= ' ,G15.6,T82,'FT/SEC',/
 810  *      ,T58,UBR= ' ,G15.6,T82,;FT/SEC,;G15.6,T58,FT/SEC,;G15.6,T82,
 820  *      ,T58,VB,VC,VE
  FORMAT(6,820) VB,VC,VE
  *      ,T58,VB=G15.6,T82,'CUBIC IN.,/,T58,VE=G15.6,T58,
 820  *      ,VCE=G15.6,T82,'CUBIC IN.,/,T58,VE=G15.6,T82,
  *      ,CUBIC IN.)
  GO TO 850
  WRITE(6,840) VOID
  FORMAT(6,840) VOID,T58,VOID=' ,G15.6
  IF(H.GE.12.0*HF) GO TO ' ,G15.6
  I=I+1
  INDEX=INDEX+1
  CONTINUE
 900  WRITE(6,910) HTOTAL
 905  FORMAT(0,T52,0,TOTAL BED HEIGHT= ' ,F7.2,T78,'IN. ')
  GO TO 950
 940  WRITE(6,942)
 942  FORMAT(0,T40,MODEL LIMITS EXCEEDED-XM.GE.2.0-CHECK DIAI AND
  *      GMF)
  GO TO 9000
  ****RESULTS OF MODEL LIMIT TESTS ****
 945  WRITE(6,946)
 946  FORMAT(0,T40,MODEL LIMITS EXCEEDED-UBREL.LE.UMFCGS/EMF-
  *      *CHECK DIAI AND GMF,)
  GO TO 9000
 948  WRITE(6,949)
 949  FORMAT(0,T40,UTERM EXCEEDED')
  GO TO 9000
  ****CONCENTRATION SEARCH LOOP ****
 950  CGB(N)=CGUESS
  UVOL=U*AREA
  VZERO=0.523599*DIAR**3
  ICOUNT=1
  JCOUNT=1
  KCOUNT=1

```



```

LCOUNT=1
MCOUNT=1 NCOUNT=1,20
DO 6000 NCOUNT=1,20
IF (ICOUNT.EQ.1) GO TO 990
IF (ICOUNT.EQ.2) GO TO 980
IF (ICOUNT.EQ.1) GO TO 975
GMAX=CGB(N)
CGB(N)=GMIN+0.62*(GMAX-GMIN)
GO TO 995
GMIN=CGB(N)-DELG
CGB(N)=GMIN+0.62*(GMAX-GMIN)
GO TO 995
GMIN=CGB(N)
IF (JCOUNT.EQ.1) GO TO 985
CGB(N)=GMIN+0.62*(GMAX-GMIN)
GO TO 995
CGB(N)=CGB(N)+DELG
GO TO 995
GMIN=CGB(N)
RMAX=RZERO/12.0
RMIN=0.0000
IF (NCOUNT.EQ.1) GO TO 1055
1000 WRITE('6:1050') NCOUNT
1050 FORMAT('0:T59', 'TRIAL NUMBER= ', I3)
GO TO 1059
1055 WRITE('6:1056') NCOUNT
1056 FORMAT('1:T59', 'TRIAL NUMBER= ', I3)
1059 CGBN=CGB(N)
WRITE('6:1060') CGBN
1060 FORMAT('0:T66', 'CGB(N)= ', G15.8)
IF (LABEL.EQ.1) GO TO 1080
1061 WRITE('6:1061') GO TO T30, 'RESULTS OF TRIAL AND ERROR SEARCH'
1061 * FOR RCURE IN TOP SECTION
1065 WRITE('6:1070') 'JOB', 'TEST', 'CONSTANT', T42,
1070 FORMAT('0:T5', 'RHO')
1080 CONTINUE
L=N
DO 5000 J=1,N
TEST=0
JOB=1
IPRINT=1

```



```
IF(J.NE.1) GO TO 4000
      **** RCORE SEARCH LOOP ****
```



```

FLOW=UVOL*CGB(L)
XFLOW=GEX(L)*(CGE(L)-CGB(L))
REACT=CSR(L)*CONS*CGB(L)
CGB(L-1)=(FLOW-XFLOW+REACT)/UVOL
VCORE=4*18879*TEST**3
CS(L)=VCORE*CS0/
COEF1=(UVOL*B)*(CG0-CGB(L-1))
COEF2=WFEED*D*DENS
COEF3=WFEEL*L)*CS(L)
TEST1=(GUEF2+C0EF3-C0EF1)/WB(L-1)
TEST2=(WB(L-1)-CS(L-1)*CS(L)-WFEED*CS(L))/DENS
TESTA=TEST1-TEST2
RHO=DABS(BETA)
WRITE(6,3500) JOB, RTEST, CONS, RHO
3500 FORMAT(6,0,15,3615,5)
FORMAT(6,3600,TEST1,TEST2
3600 FORMAT(6,0,15,TEST1=620,6,T40,'TEST2= ',G20.6)
IF(TEST1.EQ.0.0) GO TO 3900
IF(TEST1.EQ.0.0) TEST1=1
VALUE1=DABS(TEST1)
VALUE2=DABS(TEST2)
IF(VALUE1.GT.VALUE2) GO TO 3800
IF(RHO/VALUE1.LE.1.0E-4) GO TO 4900
GO TO 3900
IF(RHO/VALUE2.LE.1.0E-4) GO TO 4900
3900 JOB=JOB+1
GO TO 1150
4000 IF(J.EQ.N) GO TO 4500
C*****
C*****MIDDLE SECTION MATERIAL BALANCES
C*****C
VCORE=CS(L)*VZERO/CS0
RTEST=(VCORE/4*18879)**(1.0/3.0)
CONS=24*0*RTEST**2*RATEK/DIAR**3
CGE(L)=GEX(L)*CGB(L)/(GEX(L)+ESR(L)*CONS)
TSR=ESR(L)+CSR(L)
CGBAR(L)=(CSR(L)*CGB(L)+ESR(L)*CGE(L))/TSR
CNORM(L+1)=CGBAR(L)/CGBAR(L)
PROD(L)=TEST(L)*CGBAR(L)
FLOW=UVOL*CGB(L)
XFLOW=GEX(L)*(CGE(L)-CGB(L))
REACT=CSR(L)*CONS*CGB(L)
CGB(L-1)=(FLOW-XFLOW+REACT)/UVOL
FACT1=(UVOL*B)*(CG0-CGB(L-1))
FACT2=WFEED*D*DENS+WE(L)*CS(L)
CS(L-1)=(FACT2-FACT1)/WB(L-1)

```


GO TO 4900


```

      IF(MCOUNT.EQ.1) GO TO 5900
5820  ICOUNT=2
      KCOUNT=KCOUNT+1
      MCOUNT=2
      GO TO 6000
      ICOUNT=1
      JCOUNT=1
      KCOUNT=1
      MCOUNT=1
      CONTINUE
      6000
C*****DATA OUTPUT FORMAT *****
C*****FORMAT(*,1,T48,J,SECTION RESIDENCE TIMES //(''0'',6(I4,G1
C*****FORMAT(*,6.5))
      7050  WRITE(6,7050)(L,TRES(L),L=1,N)
      7050  FORMAT(*,1,T48,J,SECTION RESIDENCE TIMES //(''0'',6(I4,G1
      *6.5))
      7200  WRITE(6,7200)(J,CGB(J),J=1,N)
      7200  FORMAT(*,0,T42,J,SECTION BUBBLE PHASE GAS CONCENTRATION
      * /(*,6(I4,G16.5)))
      7250  WRITE(6,7250)(J,CGE(J),J=1,N)
      7250  FORMAT(*,0,T40,J,SECTION EMULSION PHASE GAS *
      * CONCENTRATION(*,0*,6(I4,G16.5)))
      7300  WRITE(6,7300)(J,CS(J),J=1,N)
      7300  FORMAT(*,0,T47,J,SECTION SOLID CONCENTRATION//(''0'',6(I4
      *G16.5)))
      7400  WRITE(6,7400)(J,WB(J),J=1,N)
      7400  FORMAT(*,0,T50,J,BUBBLE PHASE SOLIDS FLOW//(''0'',6(I4,
      *G16.5)))
      7450  WRITE(6,7450)(J,WE(J),J=1,N)
      7450  FORMAT(*,0,T49,J,EMULSION PHASE SOLIDS FLOW//(''0'',6(I4,
      *G16.5)))
      7500  WRITE(6,7500)(J,GEX(J),J=1,N)
      7500  FORMAT(*,0,T50,J,GAS EXCHANGE COEFFICIENT//(''0'',6(I4,
      *G16.5)))
      7550  WRITE(6,7550)(J,ESR(J),J=1,N)
      7550  FORMAT(*,0,T50,J,EMULSION SOLIDS RATIO//(''0'',6(I4,G16
      *5)))
      7600  WRITE(6,7600)(J,CSR(J),J=1,N)
      7600  FORMAT(*,0,T50,J,CLOUD SOLIDS RATIO//(''0'',6(I4,G16.5)))
      7650  WRITE(6,7650)(J,XNB(J),J=1,N)
      7650  FORMAT(*,0,T45,J,NUMBER OF BUBBLES//(''0'',6(I4,G16.5)))
      7700  WRITE(6,7700)(J,RCORE(J),J=1,N)
      7700  FORMAT(*,0,T45,J,AVERAGE CORE RADIUS//(''0'',6(I4,G16.5)))
      *6(I4,G16.5))
      WRITE(6,7800)(J,CGBAR(J),J=1,N)

```



```

7800 FORMAT('0. ',T42,' AVERAGE GAS CONCENTRATION / (''0'',
* 6(14,616.5))
NTOTAL=N+1
WRITE(6,7850)(J,CNORM(J),J=1,NTOTAL)
    WRITE(6,7850)(J,NORMALIZED AVERAGE GAS CONCENTRATION
* FORMAT('0.',T42,')')
* 6(14,616.5))
    WRITE(6,7860)(J,CNORM(J),J=1,NTOTAL)
    FORMAT(6,7860)(J,NORMALIZED HEIGHT,)'0.,6(14,616.5))
C***** CALCULATION OF OVERALL CONVERSION FROM
C***** BACK MIXED EQUATIONS
C***** CONTINUE
C***** SUMTRE=0.0
C***** SUMPRO=0.0
DO 8000 L=1,N
    SUMPRO=SUMPRO+PROD(L)
    SUMTRE=SUMTRE+TRES(L)
    CONTINUE
CGBED=SUMPRO/SUMTRE
TAUBED=(DENSR*DIAr/WTMOL)/(2.0*RATEEK*CGBED*B)
TREBED=XLBSS/WFEED
RATIO=TREBED/TAUBED
CONBED=3.0*RATIO-6.0*RATIO**2+6.0*RATIO**3*
* ((1.0-DEX(-1.0/RATIO))
* WRITE(6,8100)CGBED,TREBED,TAUBED,CONBED
    FORMAT(6,8150,CGBED=','G15.6,',T50,TAUBED=','G15.6,
* /,T50,CONBED=','G15.6)
C***** CONVT=(CSO-CS(N))/CSO
C***** PCERR=DABS(CONVT-CONVX)
C***** PCERR=ERROR*100.0/CONVT
C***** WRITE(6,8490)RESULTS OF SEARCH ON INITIAL
C***** FORMAT(6,8500)CONVT,CONVX,ERROR,PCERR
    WRITE(6,8500)CONVT='G15.6/','T50/','O/T50','CONVEX='
* G15.6/','T50/','ERROR=';G15.6/','T50/','CONVEX='
* PCERR=';G15.6)
C***** CONTINUE
8490 * BUBBLE SIZE')
    FORMAT(6,8500)CONVT,CONVX,ERROR,PCERR
    WRITE(6,8500)CONVT='G15.6/','T50/','O/T50','CONVEX='
* G15.6/','T50/','ERROR=';G15.6/','T50/','CONVEX='
* PCERR=';G15.6)
8500 FORMAT(6,8500)CONVT,CONVX,ERROR,PCERR
    WRITE(6,8500)CONVT='G15.6/','T50/','O/T50','CONVEX='
* G15.6/','T50/','ERROR=';G15.6/','T50/','CONVEX='
* PCERR=';G15.6)
8600 CONTINUE
9000 STOP
END

```


BIBLIOGRAPHY

1. Wen, C. Y., "Noncatalytic Solid-Gas Reactions in a Fluidized Bed Reactor," Chemical Engineering Science, v. 25, p. 1395-1404, September 1970.
2. Askins, J. W., Hinds, G. P., and Kunreuther, F., "Fluid Catalyst-Gas Mixing in Commercial Equipment," Chemical Engineering Progress, v. 47, p. 401-404, August 1951.
3. Toomey, R. D., and Johnstone, H. F., "Gaseous Fluidization of Solid Particles," Chemical Engineering Progress, v. 48, p. 220-226, May 1952.
4. Shen, C. Y., and Johnstone, H. F., "Gas-Solid Contact in Fluidized Beds," American Institute of Chemical Engineers Journal, v. 1, p. 349-354, September 1955.
5. Pansing, W. F., "Regeneration of Fluidized Cracking Catalysts," American Institute of Chemical Engineers Journal, v. 2, p. 71-74, March 1956.
6. Lewis, W. K., Gilliland, E. R., and Glass, W., "Solid-catalyzed Reaction in a Fluidized Bed," American Institute of Chemical Engineers Journal, v. 5, p. 419-426, December 1959.
7. Mathis, J. F., and Watson, C. C., "Effect of Fluidization on Catalytic Cumene Dealkylation," American Institute of Chemical Engineers Journal, v. 2, p. 518-528, December 1956.
8. Massimilla, L., and Johnstone, H. F., "Reaction Kinetics in Fluidized Beds," Chemical Engineering Science, v. 16, p. 105-112, November 1961.
9. Gomezplata, A., and Shuster, W. W., "Effects of Uniformity of Fluidization on Catalytic Cracking of Cumene," American Institute of Chemical Engineers Journal, v. 6, p. 454-459, September 1960.
10. May, W. G., "Fluidized-bed Reactor Studies," Chemical Engineering Progress, v. 55, p. 49-56, December 1959.
11. van Deemter, J. J., "Mixing and Contacting in Gas-Solid Fluidized Beds," Chemical Engineering Science, v. 13, p. 143-154, February 1961.

12. McCracken, E. A., Mayer, F. X., and Spencer, E. H., paper presented at the 60th Annual Meeting, American Institute of Chemical Engineers, New York, November 1967
13. McCracken, E. A., Leefe, G. L., and Weaver, R. C., "Transient Numerical Solutions for Two-Phase Fluid-Bed Models," Chemical Engineering Symposium Series, v. 66(101), p. 37-46, 1970.
14. Davidson, J. F., and Harrison, D., Fluidized Particles, Cambridge University Press, 1963.
15. Kunii, D., and Levenspiel, O., Fluidization Engineering, Wiley, 1969.
16. Grace, J. R., "An Evaluation of Models for Fluidized Bed Reactors," American Institute of Chemical Engineers Symposium Series, v. 67(116), p. 159-167, 1971.
17. Orcutt, J. C., Davidson, J. F., and Pigford, R. L., "Reaction Time Distributions in Fluidized Catalytic Reactors," Chemical Engineering Progress Symposium Series, v. 58(38), p. 1-15, 1962.
18. Hovmand, S., and Davidson, J. F., "Chemical Conversion in a Slugging Fluidized Bed," Transactions, Institution of Chemical Engineers, v. 46, p. 190-203, 1968.
19. Partridge, B. A., and Rowe, P. N., "Chemical Reaction in a Bubbling Gas-Fluidised Bed," Transactions, Institution of Chemical Engineers, v. 44, p. 335-348, 1966.
20. Chiba, T., and Kobayashi, H., "Gas Exchange Between the Bubble and Emulsion Phases in Gas-Solid Fluidized Beds," Chemical Engineering Science, v. 25, p. 1375-1385, September 1970.
21. Kunii, D., and Levenspiel, O., "Bubbling Bed Model," Industrial and Engineering Chemistry Fundamentals, v. 7, p. 446-452, August 1968.
22. Toor, F. D., and Calderbank, P. H., Proceedings of the International Symposium on Fluidization, p. 373, Amsterdam University Press, 1967.
23. Yates, J. G., Rowe, P. N., and Whang, S. T., "The Isomerization of N-Butenes over a Fluidised Silica-Alumina Catalyst," Chemical Engineering Science, v. 25, p. 1387-1394, September 1970.

24. Kato, K., and Wen, C. Y., "Bubble Assemblage Model for Fluidized Bed Catalytic Reactors," Chemical Engineering Science, v. 24, p. 1351-1369, August 1969.
25. Kobayashi, H., Arai, F., and Shiba, T., Chemical Engineering, Tokyo, v. 29, p. 858, 1965.
26. Harrison, D., Davidson, J. F., and deKock, J. W., "The Nature of Aggregative and Particulate Fluidisation," Transactions, Institution of Chemical Engineers, v. 39, p. 202-211, 1961.
27. Davies, R. M., and Taylor, G., "The Mechanics of Large Bubbles Rising Through Extended Liquids and Through Liquids in Tubes," Proceedings of the Royal Society, v. 200, p. 375-380, 1950.
28. Nicklin, D. J., "Two-phase Bubble Flow," Chemical Engineering Science, v. 17, p. 693-702, September 1962.
29. Davidson, J. F., "Symposium on Fluidisation-Discussion," Transactions, Institution of Chemical Engineers, v. 39, p. 223-240, 1961.
30. Rowe, P. N., and Partridge, B. A., "An X-Ray Study of Bubbles in Fluidised Beds," Transactions, Institution of Chemical Engineers, v. 43, p. 157-177, 1965.
31. Latham, R., Hamilton, C., and Potter, O. E., "Back-mixing and Chemical Reaction in Fluidised Beds," British Chemical Engineering, v. 13, p. 666-671, May 1968.
32. Kobayashi, H., Arai, F., and Sunagawa, T., Chemical Engineering, Tokyo, v. 31, p. 239, 1967.
33. Levenspiel, O., Chemical Reaction Engineering, Wiley, 1962.
34. Yagi, S., Kunii, D., Nagano, T., and Mineta, H., Journal of the Chemical Society of Japan, Industrial Chemical Engineering Section, v. 56, p. 213-215, 1953.
35. Danckwerts, P. V., "Continuous Flow Systems," Chemical Engineering Science, v. 2, p. 1-13, February, 1953.
36. Toei, R., Some Opinions for Modelling Fluidised Beds, paper presented at the 64th Annual Meeting of the American Institute of Chemical Engineers, San Francisco, California, 28 December 1971.

37. Behie, L. A., and others, "Jet Momentum Dissipation at a Grid of a Large Gas Fluidized Bed," Canadian Journal of Chemical Engineering, v. 48, p. 158-161, April 1970.
38. Yagi, S., and Kunii, D., Fifth International Symposium on Combustion, p. 231-244, Reinhold, 1955.
39. Leva, M., Fluidization, McGraw-Hill, 1959.
40. Agarwal, O. P., and Storrow, J. A., "Pressure Drop in Fluidization Beds," Chemistry and Industry (London), v. 10, p. 278-286, 14 April 1951.
41. Chemical Engineer's Handbook, 4th ed., p. 3-320, McGraw-Hill, 1963.

INITIAL DISTRIBUTION LIST

No. Copies

- | | |
|---|---|
| 1. Defense Documentation Center
Cameron Station
Alexandria, Virginia 22314 | 2 |
| 2. Library, Code 0212
Naval Postgraduate School
Monterey, California 93940 | 2 |
| 3. Professor J. H. Duffin, Code 54
Department of Material Science and Chemistry
Naval Postgraduate School
Monterey, California 93940 | 1 |
| 4. Ens. Charles Joseph Dale
517 Cherry Tree Road
Aston, Pennsylvania 19014 | 1 |

UNCLASSIFIED

Security Classification

DOCUMENT CONTROL DATA - R & D

(Security classification of title, body of abstract and indexing annotation must be entered when the overall report is classified)

1. ORIGINATING ACTIVITY (Corporate author) Naval Postgraduate School Monterey, California 93940		2a. REPORT SECURITY CLASSIFICATION Unclassified
2b. GROUP		
3. REPORT TITLE THE DEVELOPMENT AND STUDY OF A MATHEMATICAL MODEL FOR NON-CATALYTIC REACTIONS IN A FLUIDIZED BED REACTOR		
4. DESCRIPTIVE NOTES (Type of report and inclusive dates) Master's Thesis; June 1972		
5. AUTHOR(S) (First name, middle initial, last name) Charles Joseph Dale; Ensign, United States Navy		
6. REPORT DATE June 1972	7a. TOTAL NO. OF PAGES 102	7b. NO. OF REFS 41
8a. CONTRACT OR GRANT NO.	9a. ORIGINATOR'S REPORT NUMBER(S)	
b. PROJECT NO.		
c.	9b. OTHER REPORT NO(S) (Any other numbers that may be assigned this report)	
d.		
10. DISTRIBUTION STATEMENT Approved for public release; distribution unlimited.		
11. SUPPLEMENTARY NOTES	12. SPONSORING MILITARY ACTIVITY Naval Postgraduate School Monterey, California 93940	

13. ABSTRACT

A mathematical model for the simulation of non-catalytic solid-gas reactions in a fluidized bed reactor is proposed. The performance of the model in predicting solid reactant conversions for an ore roasting process is investigated using available literature data. Model development required simplifying assumptions. The sensitivity of the model to certain of these assumptions is investigated.

Comments on the adaptability of the model for use in the design and study of a fluidized bed shipboard waste disposal system are made.

UNCLASSIFIED

Security Classification

KEY WORDS	LINK A		LINK B		LINK C	
	ROLE	WT	ROLE	WT	ROLE	WT
FLUIDIZED BED						
SOLID WASTES						
SIMULATION						

FORM 1473 (BACK)
1 NOV 65

101-807-6821

UNCLASSIFIED

135038

Thesis

D1415 Dale

c.1

The development and
study of a mathematical
model for non-catalytic
reactions in a fluidized
bed reactor.

Thesis

D1415 Dale

c.1

The development and
study of a mathematical
model for non-catalytic
reactions in a fluidized
bed reactor.

135038

thesD1415
The development and study of a mathemati



3 2768 002 09493 0
DUDLEY KNOX LIBRARY